Mesopelagic sound scattering layers and possible explanations for their diel variations in Bjørnafjorden, western Norway

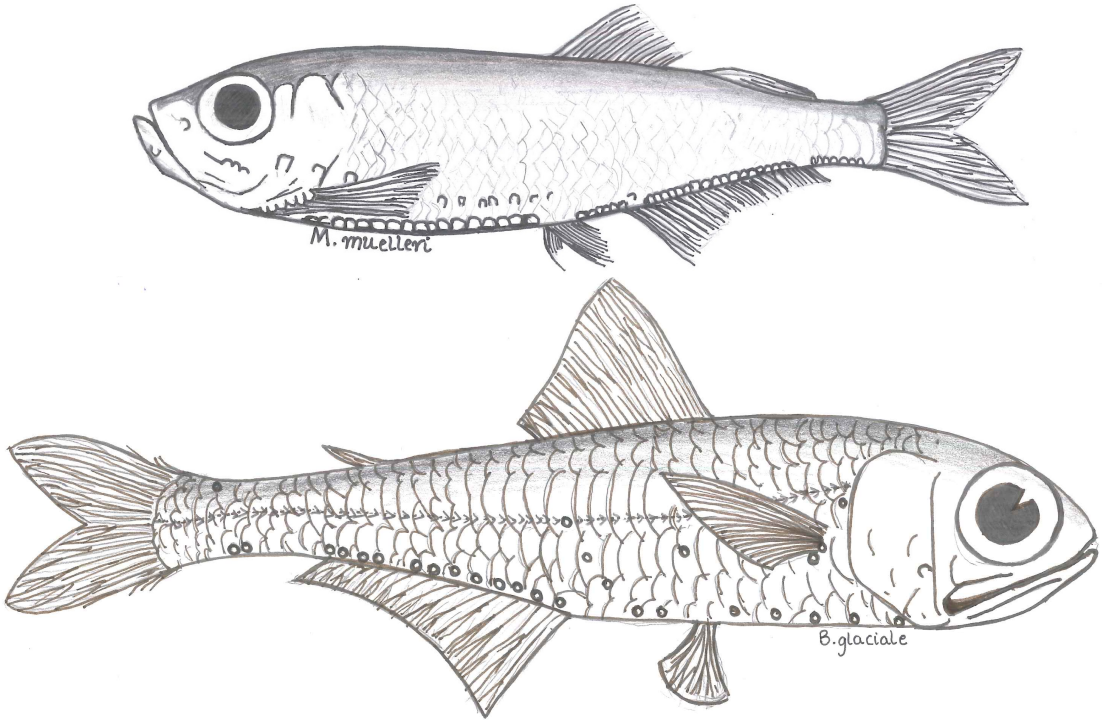

Kristine Rokke

Department of Biological Sciences

University of Bergen

November 2018

Front cover motive: *Maurolicus muelleri* and *Benthosema glaciale.* Designed by Kristine Rokke.

ACKNOWLEDGEMENTS

First of all, I would like to express my gratitude to my supervisor Dag Lorents Aksnes. He has guided be through this process with patience and encouragement, and provided me with great inputs, quick feedbacks and motivational words.

I am also grateful for the help and feedback on my thesis from my cosupervisor Anne Gro Vea Salvanes. I would also like to thank my supervisors at the Institute of Marine Research (IMR) Espen Strand and Thor A. Klevjer. Their feedbacks on the early drafts and help on managing the statistical software (R) and processing the data have been immensely helpful. I would also like to thank Knut Helge Jensen and the people at R-club for further assistance in R.

Thanks to Monica Martinussen at the IMR for helping me out and guiding me at the lab, and for always being available and assisting me when needed.

I am also beyond grateful for my fantastic fellow students and friends. These five years would not have been the same without you. My days as a student will soon be behind be, but with me I take unforgettable memories and friends for life.

I wish to thank my family and my dearest Even for the encouragement and support.

#Lektorlove

Bergen, November 2018

Kristine Rokke

INDEX

ABSTRACT

This thesis investigates the diel variations in mesopelagic acoustic scattering layers in Bjørnafjorden (60° 5' N 5° 23'E), western Norway. The main objective was to map these scattering layers and investigate possible explanations for their diel variations. The data on which this investigation is based was collected on a cruise directed by the Institute of Marine Research (IMR) (Knutsen, 2015: HI tokt 2015117). The cruise was conducted in Bjørnafjorden from the 15th to the 22nd of November 2015, with the research wessel G.O Sars. The data material consists of acoustic data, light measurements and light estimates, hydrographic measurements, vertical distribution of zooplankton biomass and stomach analysis and length measurements of the two mesopelagic fish species *Benthosema glaciale* (Northern lantern fish) and *Maurolicus muelleri* (Müellers pearlside).

Acoustic data revealed two distinct backscattering layers, exhibiting different diel migration patterns. The shallowest layer (SSL1) had a mean daytime distribution at ~ 100 m, while the deeper layer (SSL2) had a mean daytime distribution at ~ 170 m. The SSL1 migrated towards the sea surface at dusk, while the SSL2 migrated to deeper waters. Shortly after the individuals of the SSL1 reached the surface at dusk, they descended to ~ 50 m and stayed there until dawn. At dawn the SSL1 undertook another migration to the surface before returning to their daytime depth. This can be described as normal *diel vertical migration* (DVM) with a concurrent midnight sinking. The SSL2 stayed in the deeper waters (~230-300 m) all night before ascending to their daytime distribution, exhibiting what is known as *inverse diel vertical migration* (IDVM).

Measurements and estimates of light revealed that both the SSLs followed a preferred *light comfort zone* (LCZ) during daytime. Zooplankton biomass distribution showed that the zooplankton was mainly distributed below the depth of 150 m, overlapping the SSL2. This distribution of zooplankton might explain why the SSL2 did not migrate to the surface, but stayed at depth both day and night. Several hypotheses regarding the night time distributions of the SSLs were investigated, but no conclusions were made.

1. INTRODUCTION

The mesopelagic zone (200-1000 m) (Gjøsæter and Kawaguchi, 1980, Lam and Pauly, 2005) refers to the water masses located beneath the productive photic epipelagic and above the dark aphotic bathypelagic. It is often referred to as the twilight zone (Russell, 1931, Warrant and Adam Locket, 2004, Buesseler and Boyd, 2009) and is characterized by having just enough light for animals with light sensitive eyes to see, but not enough for photosynthesis (Moku et al., 2000).

A ubiquitous feature of the mesopelagic ocean is its dense acoustic backscattering layers known as *sound scattering layers* (SSL´s) or *deep scattering layers* (DSL´s). These scattering layers were first detected in the 1940s during WWII (Kampa and Boden, 1954), and they are present in all the world´s oceans and can be detected and tracked by acoustic echo sounders (Marshall, 1951). Acoustic surveys have revealed distinct vertical migrations carried out by the individuals constituting the SSLs (Giske et al., 1990), and this behaviour is commonly referred to as *diel vertical migration* (DVM) (Hays, 2003). This is a diel recurrent event where individuals ascend to the epipelagic at dusk to feed, and descend again to the mesopelagic at dawn keeping a deeper day distribution (Røstad et al., 2016). This phenomenon is common in both freshwater and marine habitats (Lampert and Sommer, 2007), and is carried out by organisms from a diverse group of taxa, for instance jellyfish (Dupont et al., 2009), zooplankton (Lampert, 1989) and mesopelagic fish (Kaartvedt et al., 2012).

Mesopelagic fish have received much attention the past years. They serve as important trophic links and provides connectivity between plankton and top predators. They are also known to be important contributors to the transport of organic matter from the epipelagic to the mesopelagic (Merrett and Roe, 1974, Irigoien et al., 2014). The carbon assimilated when foraging in the surface is transported to the deeper layers and released through respiration and excretion (Olivar et al., 2017), thereby accelerating the carbon flux by active transport. Based on findings from the circumglobal Malaspina expedition, Irigoien et al. (2014) suggests that mesopelagic fishes, through their carbon transport, may be responsible for respiring up to ~10% of primary production in deep waters, and that the migration pattern of these

mesopelagic fishes could be a partial explanation for the large microbial respiration, and the consecutive oxygen depletion, in the deep oceans.

The global biomass of mesopelagic fish species is therefore a question of great importance when it comes to how we see their roles in the ecosystems, biogeochemical cycles and as a potential resource. A good estimate has proven hard to find, and there is still great uncertainty. Estimates based on trawling and catches from net sampling suggested a global biomass of 1 Gigatonn (Gt) (Gjøsæter and Kawaguchi, 1980). Based on new knowledge, most scientists now agree that this is an underestimate. Kaartvedt et al. (2012) reported evidence that a common myctophid fish in the North Atlantic, i.e *Benthosema glaciale*, exhibited an efficient trawl avoidance, and reasoned that other mesopelagic fish might exhibit similar avoidance of sampling nets. Irigoien et al. (2014) suggested that the global biomass might be as high as ~11 - 15 Gt, over one order of magnitude higher than the previous estimate. This estimate is a result of combined sensitivity analysis and modelling of the acoustic data from the previous mentioned Malaspina expedition. However, in that specific analysis the backscatter is attributed 100% to fish, and Proud et al. (2018) argues that this might be an inaccurate assumption leading to a higher estimation, as acoustic energy is not consistently directly proportional to fish biomass.

The ultimate causation for DVM has been explained as an evolutionary strategy for optimizing the trade-off between food intake and predation risk (Clark and Levy, 1988), and thereby maximising fitness. It has been suggested that the mesopelagic organisms comprising the SSLs seems to actively avoid too strong or too low light intensities (Røstad et al., 2016). They are said to occupy a *light-comfort zone* (LCZ) (Dupont et al., 2009, Røstad et al., 2016), with light intensities usually spanning over several orders of magnitude (Røstad et al., 2016, Roe, 1983, Staby and Aksnes, 2011, Prihartato et al., 2015). In the crepuscular hours, when light intensities in the ocean´s epipelagic are within the LCZ, organisms of the SSL can ascend to the epipelagic and forage at reduced predation risk, in comparison to the daytime risk. This is known as the *antipredation window,* and is one of the theories explaining DVM as an evolutionary behaviour (de Busserolles et al., 2017, Clark and Levy, 1988). Following the predictions of LCZ hypothesis, the SSL is expected to have a shallower weighted mean daytime depth (WMD) and a narrower depth zone correlated with a higher light attenuation in the water column (Røstad et al., 2016).

Not all mesopelagic organisms perform DVM, and the extent of the vertical migration, both in time and space, varies with season and locations, but also between and within species (Pearre, 2003, Scheuerell and Schindler, 2003). A recent study (Klevjer et al., 2016) based on the findings from the circumglobal Malaspina expedition showed that vertical migrations of the acoustic SSLs were evident in all oceans, but to a varying degree. They found that on average ~50% of the SSL made diel vertical migrations, but the estimates ranged from ~20% in the Indian Ocean to ~90% in the Eastern Pacific.

The driving forces behind the vertical distribution of the SSL and consequently also the variations in DVM has been of interest ever since the SSL was first detected in the 1940s (Kampa and Boden, 1954). Variations in surface light and light attenuation in the water column have been proposed as a proximate explanation, and is still an acknowledged hypothesis supported by several studies (Kampa and Boden, 1954, Baliño and Aksnes, 1993, Staby and Aksnes, 2011, Aksnes et al., 2017). A recent study by Bianchi et al. (2013) proposed that oxygen levels could be a controlling factor for the daytime distribution, and showed that low oxygen levels at midwater depths were correlated with shallower migration depths. They also noted that this is the best single predictor for migration amplitude on a global scale. Studies based on data from the Malaspina expedition (Klevjer et al., 2016) also found a strong correlation between weighted mean daytime depth (WMD) and levels of oxygen, but additionally found that backscatter was present deep into both hypoxic and anoxic areas, suggesting that avoidance of hypoxic waters cannot be the overall controlling factor for a shallower WMD. Aksnes et al. (2017), on the other hand, argued that the correlation between oxygen levels and migration amplitude could be explained as a negative relationship between light attenuation and levels of oxygen. Further, several other modifying factors have been suggested, including predation risk (Kahilainen et al., 2009), prey density (Neilson and Perry, 1990), hunger (Pearre, 2003) and tide (Bennett et al., 2002).

Glacier lanternfish *Benthosema glaciale* (Reinhardt, 1837) from the Myctophidae family and Müller´s pearlside *Maurolicus muelleri* (Gmelin, 1789) from the Sternoptychidae family are both small luminous fish species that inhabit the mesopelagic water masses, and make up an important part of mesopelagic fish community (Olivar et al., 2017). They are two of the most prevailing fish species in the fjords of western Norway (Kaartvedt et al., 2012, Giske et al., 1990), and serve as important planktivores, but also prey for larger fish such as saith

Pollachius virens, salmon *Salmo salar* and blue whiting *Micromesistius poutassou* (Rasmussen and Giske, 1994), making them important trophic links in the food web.

The Myctophidae family can be found in all world oceans, and is the most widespread and species rich mesopelagic fish family (Moser and Ahlstrom, 1974). *B. glaciale* is the most common species in the North Atlantic (north of about 35^{o}), western Greenland and in the Norwegian seas (Halliday, 1970, Gjøsæter, 1973a). *M. muelleri* is likewise evidently widespread around the world´s oceans (Gjøsæter, 1981). Both species are short-lived and small, but differ to some extent. Halliday (1970) found that *B. glaciale* lived to be at least 4½ years outside the east coast of Canada, reaching a maximum length of 68 mm. He further noted that greater maximum lengths and longer life-spans are attained further north, which was also verified by Gjösæter (1973a) who described a specimen from Korsfjorden, Norway, that was calculated to be 103 mm before preservation, and approximately 7-8 years old. *M. muelleri* rarely measures over 50 mm, though its maximum size is 70 mm. Only a few individuals live to the age of 3 in Norwegian waters (Gjøsæter, 1981). Thus, making *B. glaciale* a larger and longer-lived fish species than *M. muelleri.*

Within a population vertical migration patterns and depth distribution during day and night time can vary between different ontogenetic stages (Giske et al., 1990, Baliño and Aksnes, 1993, Staby and Aksnes, 2011). Giske et al. (1990) studied the vertical distribution of zooplankton and mesopelagic fish in Masfjorden, in western Norway. They found two sound scattering layers containing *M. muelleri*, where the top layer consisted of juvenile fish, and the deeper layer mainly consisted of adult fish. Dypvik et al. (2012b) studied the migration patterns of *B. glaciale* in the same fjord and found that a percentage of the population performed regular DVM, another percentage stayed in the deeper layers and a third performed what is known as inverse DVM, ascending to the surface layers at dawn. They also found in this study that the daytime distribution of *M. muelleri* and *B. glaciale* differed. *M. muelleri* is most prominent between 150 to 200 m, while *B. glaciale* dominates deeper than ~ 200 m (Kaartvedt et al., 2009).

The feeding ecology of both *B. glaciale* and *M. muelleri* consist of a variety of zooplankton (Gjøsæter, 1973b, Gjøsæter, 1981, Giske et al., 1990, Sameoto, 1988). For *B. glaciale* in Norwegian fjords, calanoid copepods of the genus *Calanus*. seems to be the preferred prey, followed by euphausiids (Gjøsæter, 1973b). For *M. muelleri* copepods seems to be the most

important prey for individuals >20 mm, while copepods and euphausiids were equally important for larger individuals (Gjøsæter, 1981). The vertical distribution of zooplankton tends to vary with season. During spring and summer, zooplankton is at its highest abundance in the surface layers (Rasmussen and Giske, 1994). As primary production starts to decline in late summer, so does the abundance of zooplankton. *Calanus spp.* is known to carry out seasonal vertical migrations, descending to mid-waters in autumn, entering a state of hibernating, known as overwintering (Hirche, 1996, Bagøien et al., 2001). From early autumn to early spring the major proportion of zooplankton is located beneath 150 m (Giske et al., 1990, Bagøien et al., 2001, Baliño and Aksnes, 1993).

Few studies have investigated the diel variations in mesopelagic migration patterns in relation to measurements of change in incoming surface irradiance, attenuation of light in the water column, vertical distribution of zooplankton biomass, trawl catches and stomach content in mesopelagic fish. In November 2015, from the 14th to the 22nd, a cruise (Knutsen 2015: Hi tokt 2015117) conducted in Bjørnafjorden, western Norway, by the Institute of Marine Research (IMR), collected such data. Acoustic data detected two sound scattering layers at different depths (SSL1 & SSL2). The mesopelagic fish species *Benthosema glaciale* and *Maurolicus muelleri* are believed to constitute essential parts of these observed acoustic scattering layers, and the SSLs will therefore be investigated accordingly in this thesis.

Concurrent measurements of surface irradiance were made, as well as two casts of light measurements in the water column. Based on these measurements, estimations of extinction coefficients (K) as well as ambient irradiance at depth were made. These observations allow for testing of different hypothesis, such as expectations related to the light comfort zone hypothesis (LCZ). The scattering layers are expected to follow a LCZ, performing vertical migrations at dusk and dawn. They are also expected to respond to immediate changes in incoming surface irradiance, i.e cloud cover, and adjust their vertical position accordingly.

In addition to light the SSLs will also be investigated in relationship to hydrographical properties (temperature, oxygen levels, salinity, nitrate and chlorophyll *a*), vertical distribution of zooplankton biomass, and stomach analysis (level of fullness and level of digestion) and length distribution of the fish species *Benthosema glaciale* and *Maurolicus muelleri.* The stomach analysis may be important in determining whether the species eat at specific times, and if so, when. In combination with the acoustic data, their position in the

water column when feeding can also be determined. This can again be compared to the vertical distribution of zooplankton. These observations will be discussed and compared to previous findings, as well as allow for new findings and hypothesis to be made.

The objective of this thesis will be to map the diel variations in the acoustic mesopelagic scattering layers and possible reasons for this, in Bjørnafjorden.

.

2. METHOD AND MATERIALS

2.1 Study area

The data material for this thesis was collected on a cruise with the research vessel G.O Sars from the 14th of November to the 21th of November 2015 in Bjørnafjorden (Knutsen 2015: Hi tokt 2015117). The cruise was a methodologically focused cruise with the purpose of testing quantitative sampling methods for macroplankton and micronekton. Bjørnafjorden (Figure 1) is a fjord in Hordaland, Norway (60° 5' N 5° 23'E), located 40 km south of Bergen. It has a maximum depth of approximately 600 meters. The data material consists of hydrographic measurements, light measurements, acoustic data, as well as samples of zooplankton and the two mesopelagic fish species; *Benthosema glaciale* (Northern lantern fish) and *Maurolicus muelleri* (Müellers pearlside).

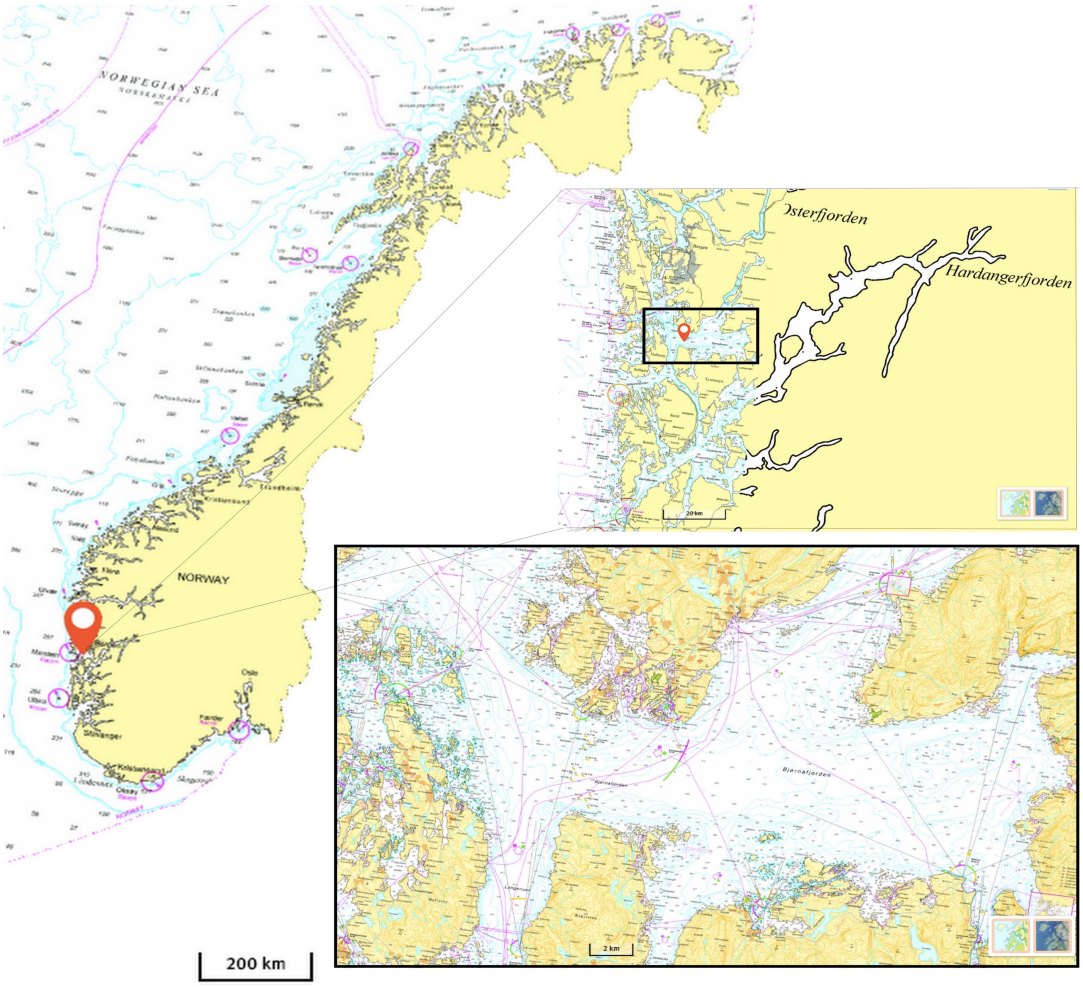

Figure 1. Map of Bjørnafjorden. Made with, and retrieved from https://www.kartverket.no/kart/sjokart/

2.3 Hydrographic measurements

A Sea-Bird SBE 9 CTD was used for measuring the physical properties of the water column in Bjørnafjorden. A CTD measures conductivity, temperature and depth, and calculates salinity based on the electrical conductivity measurements. In addition to these measurements an auxiliary oxygen sensor was mounted on the CTD. The CTD was lowered vertically with a speed of 0.5 m s^{-1}, and data was registered every meter. This gives a good profile of the water column. Three CTD-stations were taken in Bjørnafjorden (Table 1), where temperature is given in degrees Celsius, oxygen in ml l^{-1} and salinity in PSU (Practical Salinity Unit).

Table 1. An overview of the CTD stations with maximal lowering depths and bottom depths.

DATE Nov 2015	STATION	Latitude	Longitude	CTD depth (m)	Bottom depth (m)
15	**420**	**60 07.52 N**	**005 35.94 E**	**466**	**475**
19	**423**	**60 07.42 N**	**005 34.14 E**	**406**	**404**
20	**424**	**60 07.17 N**	**005 34.34 E**	**480**	**493**

2.4 Light measurements

For measuring the light intensity in the water column, a RAMSES spectral radiometer was used. This is a device used for measuring electromagnetic radiation. It can measure 200 different wavelengths, including wavelengths outside the visible spectre. Two casts of underwater light measurements were done. The measurements of downwelling irradiance was gridded at every 5 meters' depth. In addition to a sensor that was lowered down into the water column, there was one mounted on top of the ship. The sensor mounted on the ship continuously measured irradiance during the whole cruise, with one-minute intervals.

2.4.1 Estimation of K-values

From the two underwater measurements, the coefficient for light attenuation in the water column, K, was calculated. The light attenuation coefficient refers to how easily the medium can be penetrated by light (Baker and Lavelle, 1984), and K was estimated at a wavelength of

485 nm. This specific wavelength was chosen because it is close to the average peak sensitivity for mycthophids (*B. glaciale*) and sternoptychids (*M. muelleri*) (Norheim et al., 2016, de Busserolles et al., 2017). The K-values for each vertical depth were calculated by using the equation for light intensity at a specific depth (underwater measurements were corrected in relation to variation in surface light during the cast):

$$(1)\ E_z = E_0 e^{-Kz}$$

Here z is depth, E_z is irradiance at depth z, E_0 is irradiance just below surface and K is the attenuation coefficient for irradiance between the surface and the depth z. To be able to extract K from this equation, the natural logarithm (ln) is used.

$$(2)\ ln(E_z) = ln\ (E_0 e^{-Kz})$$

$$(3)\ ln(E_z) = ln\ (E_0) - Kz$$

$$(4)\ ln(E_z) = - Kz + ln\ (E_0)$$

Linear regression analyses of the ln-transformed models were then implemented with irradiance versus depth, and K was thereby obtained from the slope of the regression line. The measurements grouped into an upper and a lower depth layer for light attenuation, resulting in a different K for the two depth layers, from both casts (15th and 19th of November).

2.4.2 Estimation of ambient irradiance in the water column

The equation for light intensity at a specific depth (1) was used to calculate the ambient irradiance in the water column. The measured surface irradiance (E_0) at 485nm was multiplied with the exponential of the negative attenuation coefficient (K) multiplied with depth (z). The attenuation coefficient from the 15th and the 19th of November were mediated in these estimates. The K for the upper depth layer was used from 1 to 20 m, while the K for the lower depth layer was used from 21 to 500 m. In calculating the layer from 21 to 500 m, the ambient irradiance at 20 m was used for E_0. Ambient light intensities at 485 nm were calculated from 1 to 500 m at every 15 minutes, from the 15th to the 21st of November.

2.5 Macroplankton trawls

Two different macroplankton trawls were used for sampling of the two mesopelagic fish species *B. glaciale* and *M. muelleri,* one with a mouth opening of 6 x 6 m (45 m long) and one with 10x10 m (100 m long). A macroplankton trawl has regular pelagic trawl doors, and a fixed mesh size of 3 x 3 mm from the mouth opening to the cod end. Data from four different hauls will be presented. Three of the hauls were done with the 10 x10 m mouth opening, and the last one with the 6 x 6 m. Two of the hauls were done at night time (23:01-23:48, 01:47-02:56 UTC) and the other two at daytime (09:55-10:18, 12:05-13:00 UTC). The hauls were done from the surface, down to a depth of 330-442 meters (bottom depth 473 m), and then up to the surface again, a so called oblique haul. The samples from the hauls were sorted and frozen.

2.6 Length measurements and stomach analysis

The fish were later retrieved from the freezer at the Institute of Marine Reseach (IMR) and defrosted. *B. glaciale* and *M. muelleri* were both length measured and weighed. These species often lose or damage their caudal fin when sampled by trawling, and length was therefore measured in both total length and standard length. Total length is measured from the tip of the snout to the end of the tail. Standard length is measured from the tip of the snout to the last vertebra (boneknob at the tailroot), and thereby excludes the caudal fin. After this, the fish were weighed in grams with an accuracy of four decimals. 30 individuals of each species from four hauls were examined, a total of 240 individuals. Fish were also length measured (standard length) during the cruise. These measurements are used for presenting length distribution of both species, as the number of measured fish were far greater than those measured during stomach analysis at the IMR.

The defrosted individuals were then dissected and the stomachs were retrieved and weighed. After this, the stomachs were opened, and the content was taken out and weighed. The empty stomach was also weighed. The level of filling and digestion were determined by following a categorization system (Table 2) developed by the Institute of Marine Research (IMR). Stomach filling has 6 levels, while digestion has 5. The stomach content was studied under a

Modular Routine Stereo Microscope with 8:1 Zoom Leica M80. Level of digestion was decided, but identification of species or systematic groups will not be a part of this thesis. The weight of the fish and the stomach before and after opening are given in wet weight (g). The stomach content was first weighed in wet weight, then dried at 56 degrees Celsius for at least 24 hours, and then weighed as dry weight as well.

2.6.1 Statistical tests

A Wilcoxon rank sum test was used to test if there were significant differences between day and night for the level of fullness and level of digestion for the two species. This is a test suitable for data consisting of two independent groups of samples, which does not have to be normally distributed, and where both the predictor variable and the response variable is categorical. A One-way Anova was used to test the if there were differences between lengths of fish caught at day and night, and also if there were differences in catch per effort between day and night (Catch per effort was estimated by dividing the weight of the species from the net (g), by the volume (L) filtered by the net at each haul). This test is used for data consisting of a continuous response variable and one categorical predictor variable that has more than two levels. A five percent significance level was used ($P < .05$).

Table 2. The table shows the different levels of stomach filling and digestion, and is developed by the IMR.

FILLING		DIGESTION	
	Level		**Level**
Empty. Stomach completely empty, could be some water	**1**	**Digestion not started**	**1**
Very little content. So little that the stomach has to be opened to decide between level 1 and 2	**2**	**The stomach content seems completely fresh, digestion started**	**2**
Some content. It is clearly visible outside the stomach that it is not empty.	**3**	**Digestion advanced. The species can no longer be identified, but one can distinguish systematic groups**	**3**
Full. Stomach full, but not blasted	**4**	**Digestion far advanced. One can still find eyes and larger pieces of animals in the stomach content**	**4**
Blasted. The stomach is clearly expanded and tight. The content is visible through	**5**	**Digestion almost completed. The stomach content is porridge like.**	**5**
Wrenched	**6**		

2.7 Zooplankton sampling

The multiple net sampler MOCNESS (Wiebe et al., 1985) was used for sampling zooplankton at different depth intervals. The MOCNESS is computer controlled in real time and can open and close nets at depth. It has a total of nine square mouth opening nets (180 μm mesh size; 1 m^2 opening) numbered chronologically from 0 to 8. The 0-net is open during the descent and thus samples the entire water column. At the deepest point, just as retrieval starts, net 1 is opened and this also automatically closes the previous net. At pre-determined intervals during ascent a new net is opened. At the end of each net there is a cup with meshed holes called the cod end that is used to extract the biological sample when the MOCNESS is back on board. By mistake, net 1 had been equipped with a cod end with 500 μm mesh, while the remaining 7 nets had cups with the correct mesh size of 180 μm.

The ability to sample at specific depth intervals gives information about the vertical distribution of zooplankton. Two stations will be presented in this thesis, one taken at dark (17:39-18:04 UTC) and one at in daylight (10:07-10:51 UTC). They were both taken from around 400 meters' depth and up to the surface (i.e. net 1 to 8), with approx. 50 meters' intervals for each net. The samples were conserved in formalin and stored at the IMR. When the samples were retrieved, they were first rinsed with water, and then sorted in different size ranges. This was done by using sieves with mesh sizes of 180μm, 500μm, 1000μm and 2000μm. The sorted samples were then weighed in wet weight and later put back on formalin for further storage.

2.8 Acoustics

To get an estimate of the vertical distribution and volume backscatter strength (Sv (dB re 1 m^{-1})) in the water column an echo sounder SIMRAD EK60 with a split beam system was used at the frequency of 38 kHz. This frequency will predominantly show backscatter from organisms with air-filled inclusions (Proud et al., 2018), including fish with swimbladders and siphonophores. The acoustic data measured from the 15th to the 21st of November will be presented in an echogram.

3. RESULTS

3.1 Physical and chemical properties of the water column

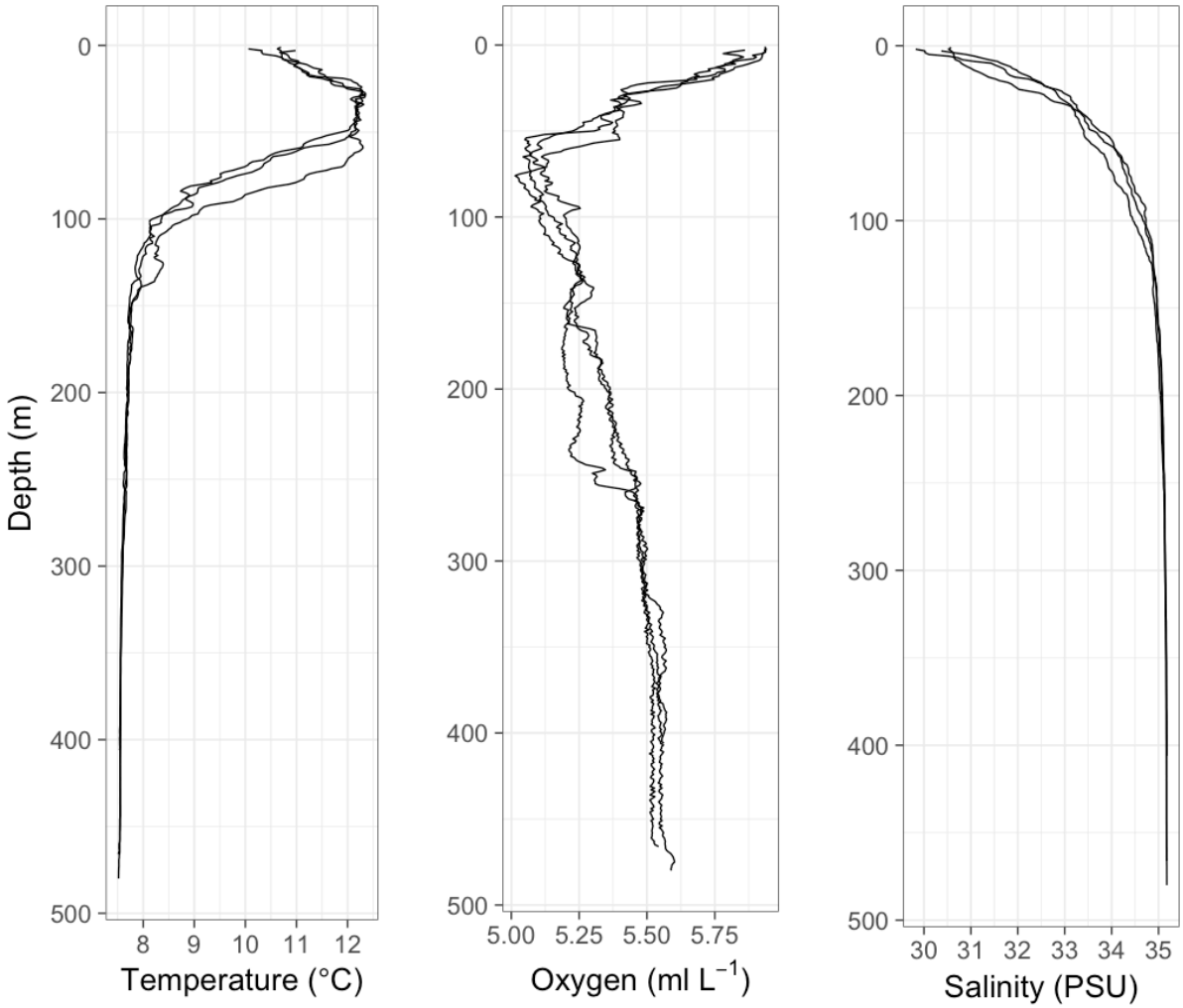

Figure 2. Temperature (°C), oxygen (ml L^{-1}) and salinity (PSU) as a function of depth. From three CTD-stations; 420, 423 and 424.

The hydrographical properties for the three stations (Table 1) revealed the same trends for temperature, oxygen and salinity (Figure 2). The surface layers measured 10 - 10.5° C, and thereafter increased to a maximum temperature at just over 12° C between 25-50 m depth. From 50 to 100 m the temperature decreased to approximately 8°C, and slowly continued to decrease to about 7.5°C at 300 m. The maximum oxygen concentration was found at the sea surface measuring around 5.87 ml L^{-1}. From the surface layers down to approx. 60 m the oxygen concentrations decreased to its lowest at 5.06 ml L^{-1} (Figure 2), suggesting a higher respiration at this depth. From 60 m to 400 m the oxygen concentration increased to 5.50 ml

L^{-1}. Salinity concentrations were lowest at the sea surface, at 30.4 PSU, and then rose to 34.75 at 100 m. From 100 to 450 m the salinity concentrations slowly continued to rise to around 35.25 PSU (Figure 2). The fjord is stratified by a warmer and less saline surface layer (approx. 50 m deep) and a deeper layer (below 100 m) that is colder and more saline. The low salinity at the surface is probably due to run-offs from rivers into the fjord.

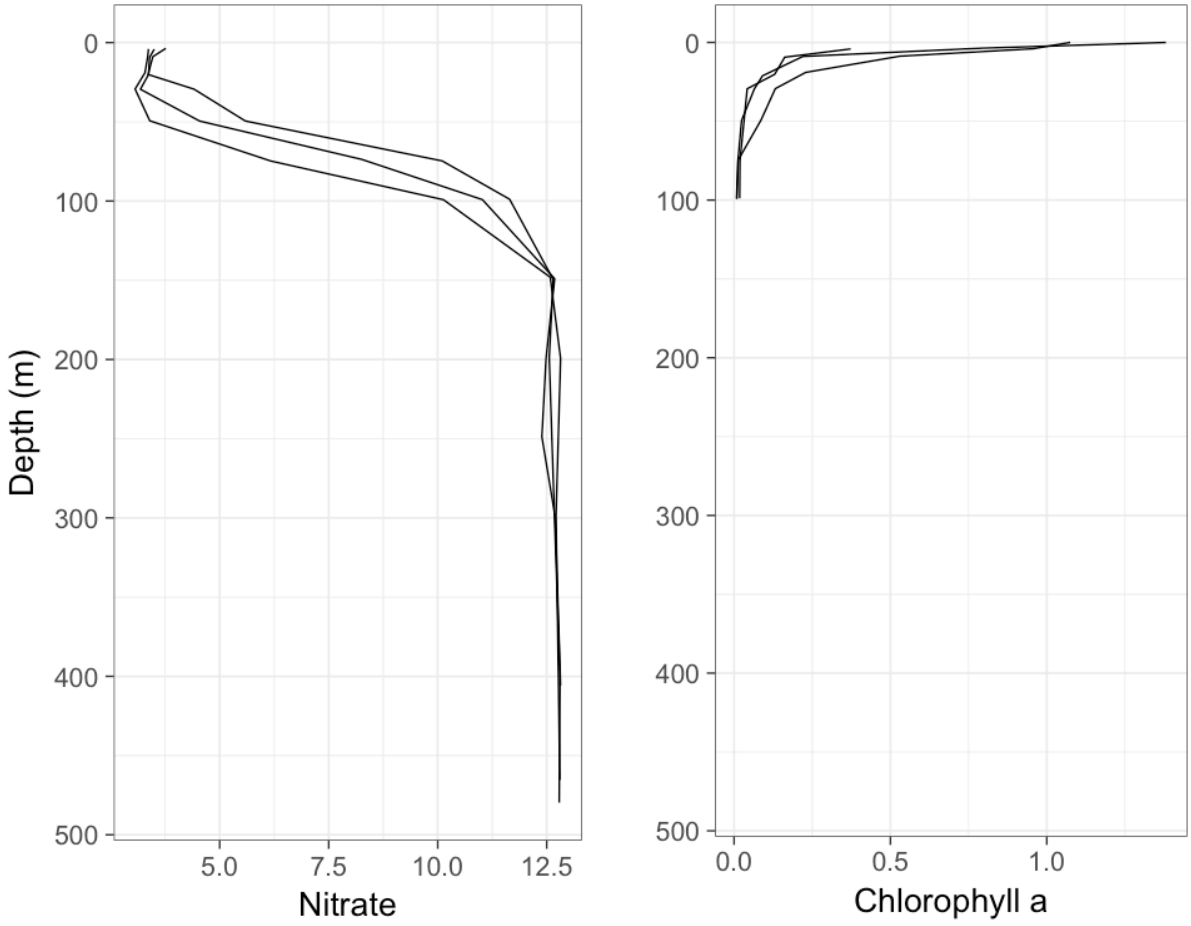

Figure 3. Concentrations of nitrate (µmol L^{-1}) and chlorophyll a (mg/m^3) as a function of depth. From three CTD-station; 420, 423 and 424.

Nitrate concentrations is lowest at the surface and down to around 50 m. It then rises and stabilizes at 150 m (Figure 3). Chlorophyll *a* concentrations is at its maximum at the surface and in the uppermost meters. It then rapidly sinks, reaching a level close to 0 mg/m^3 at 100 m (Figure 3). The correlation of an increase in nitrate and decrease in chlorophyll *a* suggests that photosynthesis is highest in the surface layer.

3.2 Measured irradiance in the water column and at the sea surface

3.2.1 Light attenuation in the water column and estimated K-values

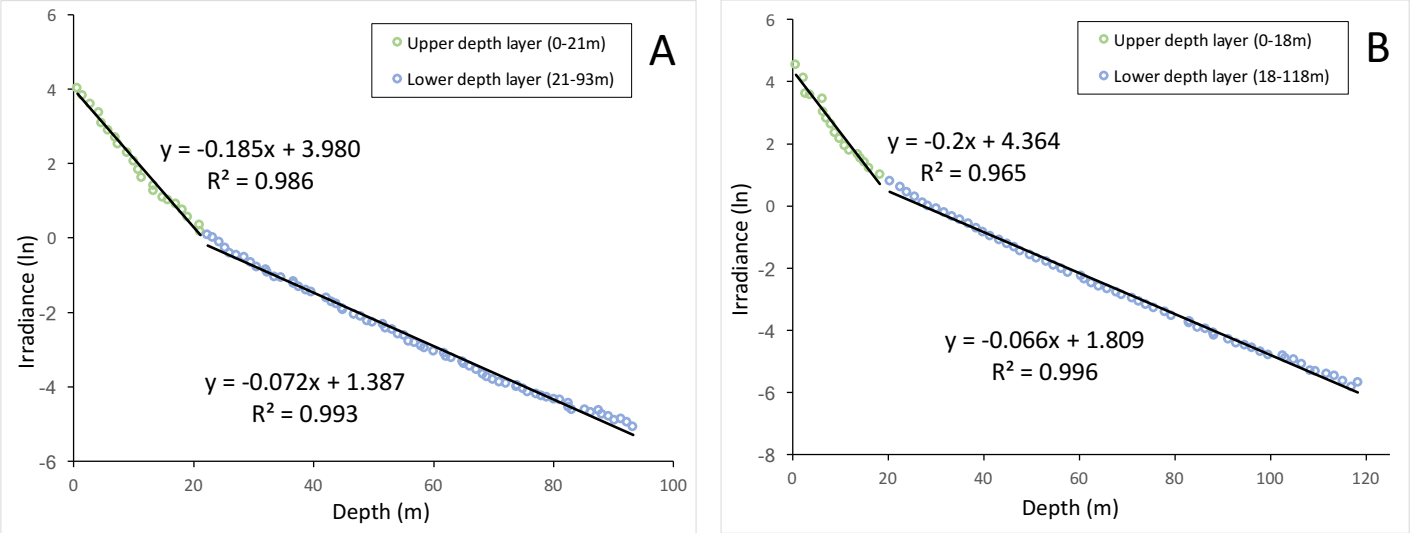

Figure 4. Downwelling irradiance at 485 nm from the 15th (A) and the 19th (B) of November 2015, with fitted linear regressions on ln-transformed measurements.

Table 3. Light attenuation coefficients (K ± 95% CI) estimated from linear regression on ln-transformed observations of downwelling irradiance (485 nm) versus depth, from Figure 4 (A) and (B).

Date (Nov 2015)	Depth layer (m)	K (m^{-1})
15 (A)	0-21	0.185 ± 0.011
	21-93	0.072 ± 0.001
19 (B)	0-18	0.200 ± 0.021
	18-118	0.066 ± 0.001

Both the measurements from the 15th and the 19th of November grouped into an upper and a lower depth layer for light attenuation, evident by the two different slopes in Figure 4. The linear regressions of the ln-transformed measurements for downwelling irradiance at 485 nm (Figure 4) reveals one order of magnitude higher attenuation values for the upper depth layer, compared to the lower depth layer (Table 3). The upper depth layers range from 0 to 21 and 0 to 18 m depth for the 15th and the 19th of November, and their estimated K-values with a 95% confidence interval (CI) 0.185 ± 0.011 m^{-1} and 0.200 ± 0.021 m^{-1}, respectively. The lower depth layers range from 21 to 93 m and 18 to118 m depth with the related K-values 0.072 ±

0.001 m^{-1} and 0.066 ± 0.001 m^{-1} (Table 3). This means that downwelling irradiance was attenuated faster in the first 20 meters of the water column compared to the deeper layers.

3.2.2 Measured surface irradiance

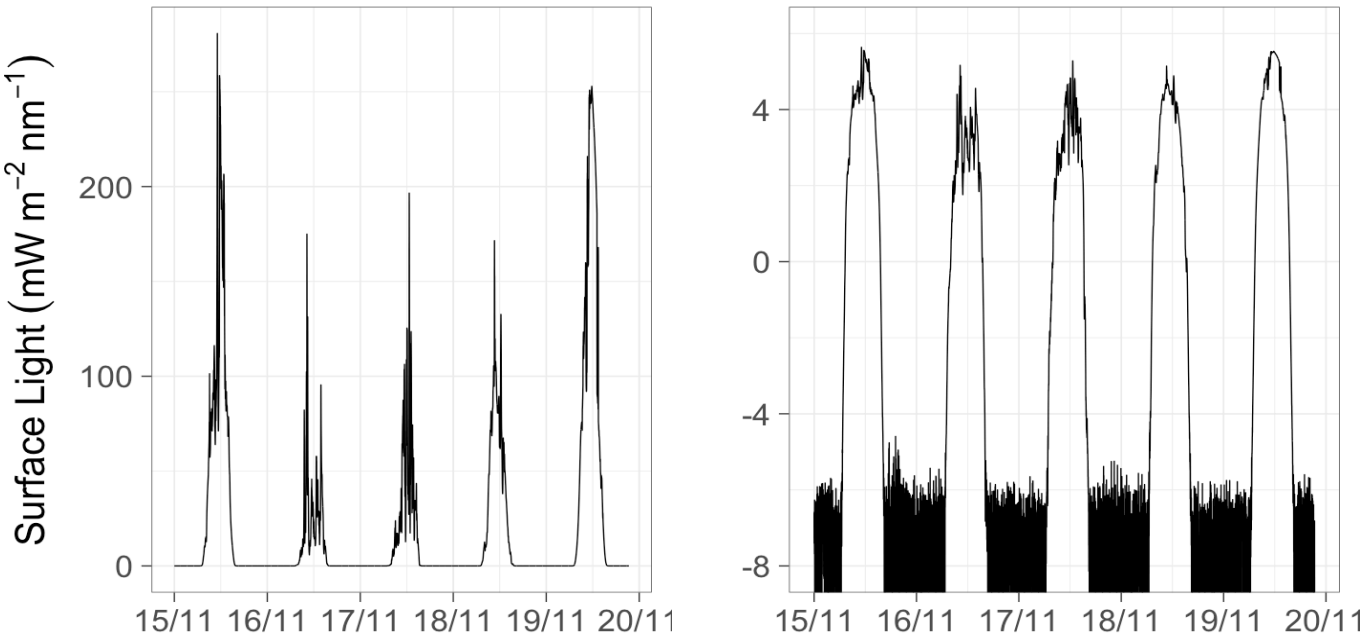

Figure 5. Surface light at 485 nm (mW m^{-2} nm^{-1}) linear (left) and logarithmic (right) from the 15th to the 20th of November 2015 as a function of time (UTC).

The maximum daytime surface irradiance at 485 nm varied from around 170 to 280 mW m^{-2} nm^{-1} over a span of 5 days (Figure 5). These variations reflect the changing cloud cover. When light intensities dropped below a certain point the radiometer was no longer sensitive enough to measure the scarce irradiance present at night time in Norway in November. This is present as noise in Figure 5 (right), and occur when the light intensities at 485 nm are less than approximately 10^{-5} mW m^{-2} nm^{-1}. Variations in night time irradiance (at 485 nm) could therefore not be measured.

3.3 Length distribution of *B. glaciale* and *M. muelleri*

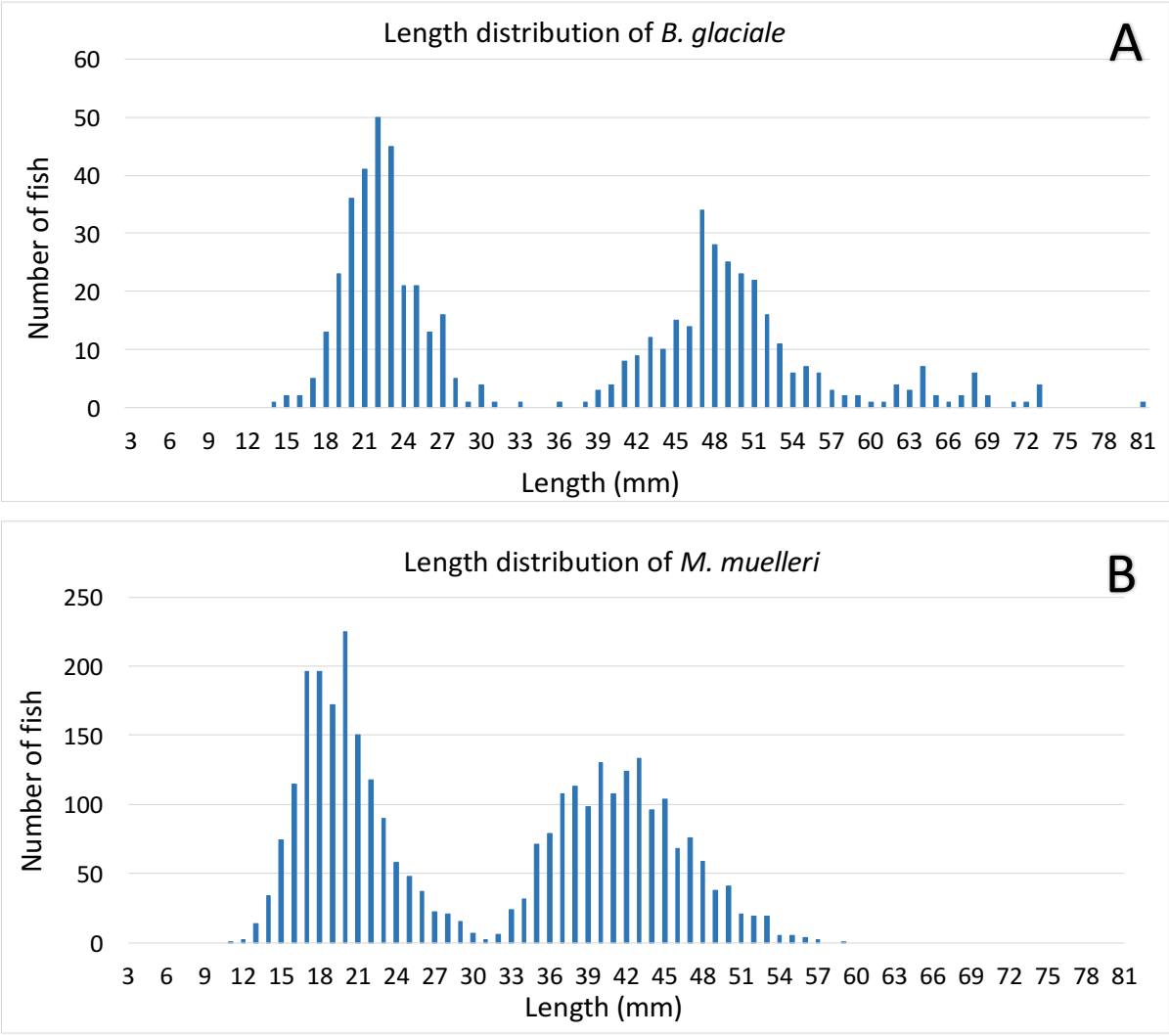

Figure 6. Length distribution of B. glaciale (A) and M. muelleri (B). Standard length measured in mm on the x-axis and number of individuals on the y-axis.

The length distribution (Figure 6) of *B. glaciale* and *M. muelleri* is based on the fish that were caught and measured during the cruise. It was a total amount of 599 individuals of *B. glaciale* and 3181 individuals of *M. muelleri*. This revealed a bimodal distribution for both species (Figure 6), suggesting two principal age classes. For *B. glaciale*, a third, older and less abundant age class also seem to be present. The age classes for *B. glaciale* can roughly be grouped into age class 1; 14-30 mm, age class 2; 39-55 mm and age class 3; > 55 mm. The two age classes for *M. muelleri* group into age class 1; 11-29 mm and age class 2; 33-53 mm. The largest specimen measured on the cruise was 81 mm for *B. glaciale*, and 59 mm for *M. muelleri*, while the smallest were 14 and 11 mm, respectively.

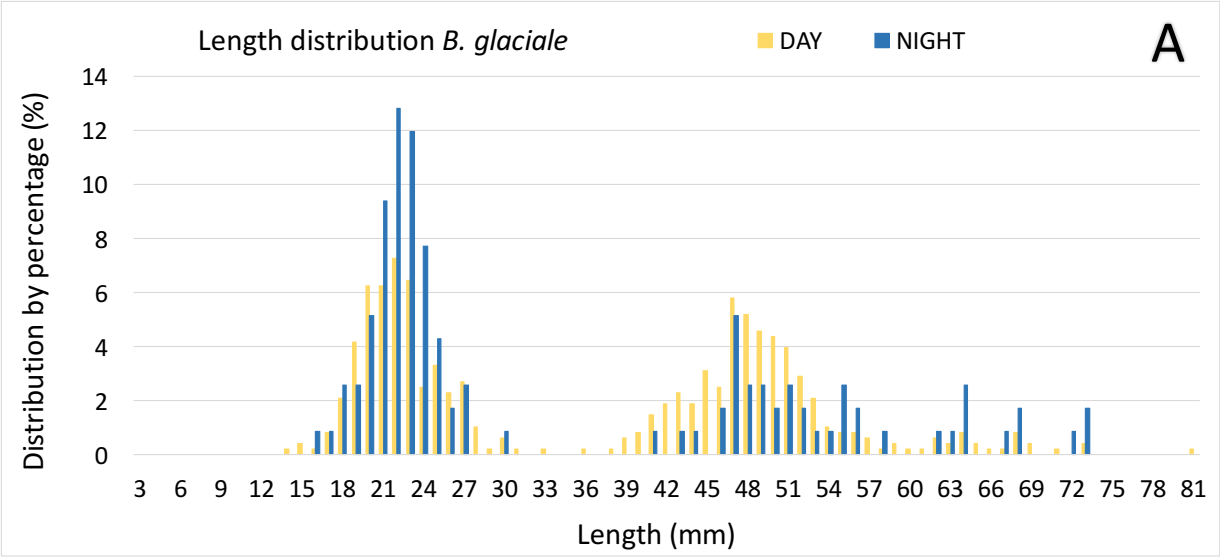

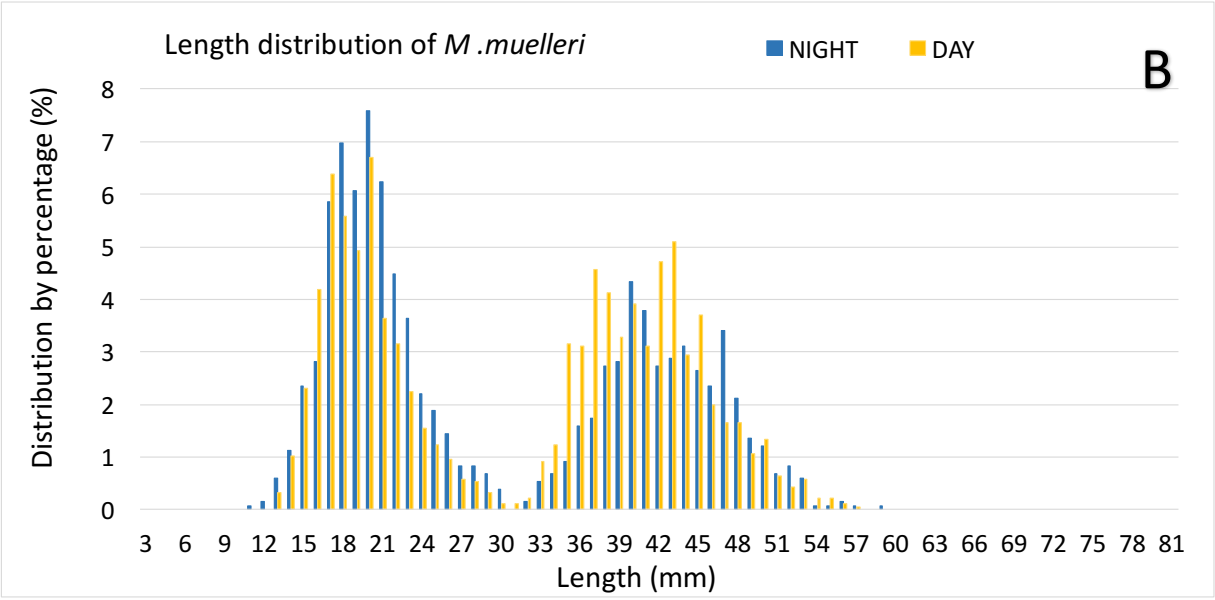

Figure 7. Length distribution of individuals caught at night versus individuals caught at day. B. glaciale (A) and M. muelleri (B). Length in mm on the x-axis and distribution by percentage on the y-axis.

Length distribution for both day- and night catches for both species (Figure 7) exhibit a bimodal pattern. It seems that there is caught more of the youngest age class and less of the older individuals of *B. glaciale* at night, compared to daytime (Figure 7A). The same trend seems to be true for *M. muelleri*, though not as prominent (Figure 7B). The aspect of catch efficiency and trawl avoidance must be considered, as this may differ between different ontogenetic stages, between day and night, and between species.

3.4 Stomach filling and digestion of *B. glaciale* and *M. muelleri*

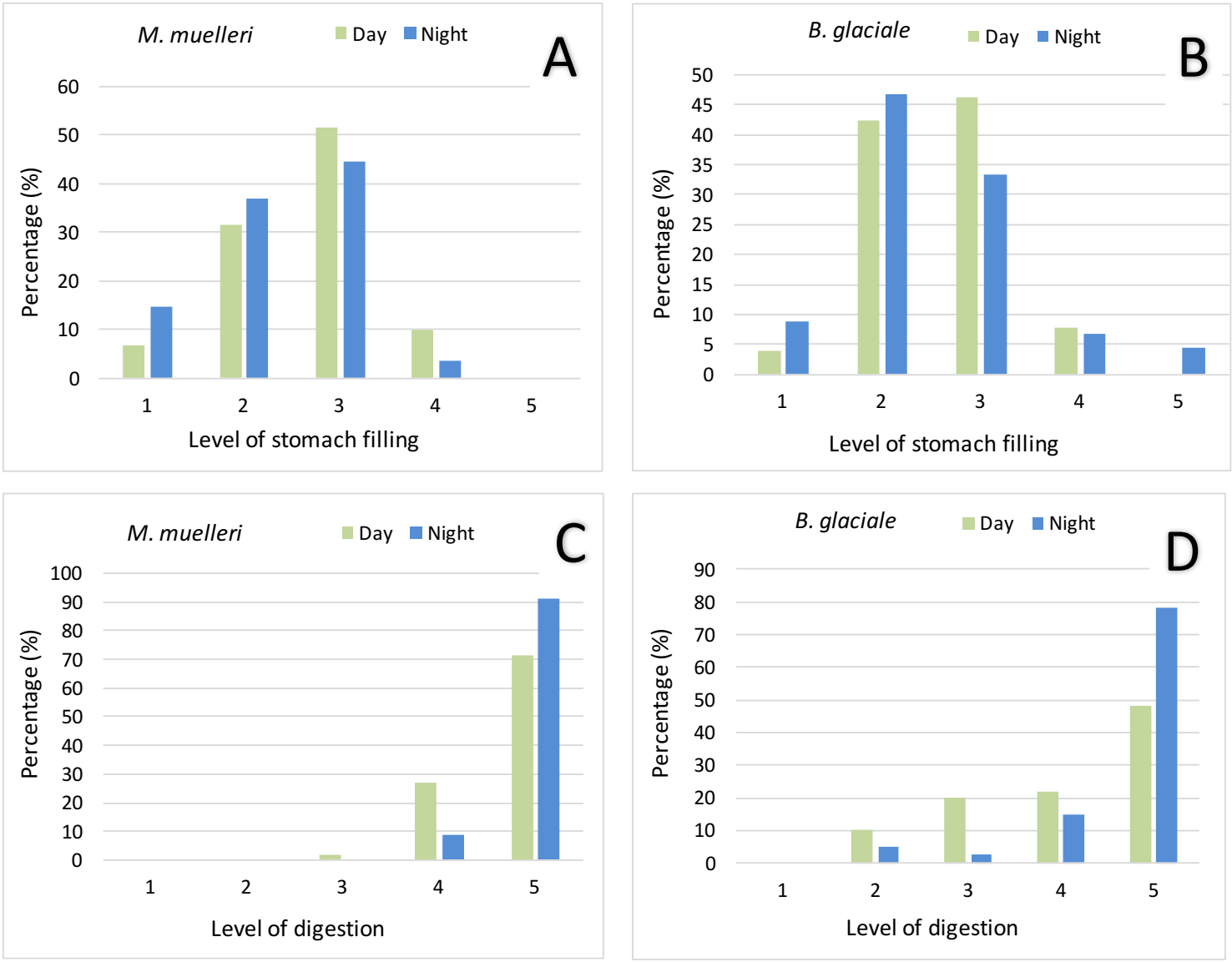

Figure 8. Distribution of stomach filling (A, B) and level of digestion (C,D) for B. glaciale and M. muelleri. With level of digestion on the x-axis and proportion of the fish dissected in percentage (%) on the y-axis.

A total of 213 individual stomachs were dissected, and the level of filling and digestion were decided (see method & materials, Table 2). The stomach filling for both species was dominated by level 2 and 3 (Figure 8 A and B), meaning that they had some content but were neither full or empty. For *B. glaciale,* level 2 and 3 combined accounted for 88.5% of the total stomachs dissected from the daytime catches, and 79.9 % from the night time catches. Likewise, for *M. muelleri*, level 2 and 3 from the daytime catches accounted for 83.2 %, and 81% for the night time catches. Level of digestion was dominated by level 5 for both species (Figure 8 C and D), meaning that the content was porridge like and that digestion was almost

complete. For *M. muelleri*, 91% of the dissected stomachs from the night time catches fell into this level 5, and equivalent 71% from the daytime catches. The same level (level 5) for *B. glaciale* amounted for 78% from the night time catches, and 48% for the daytime catches. *B. glaciale* had a higher percentage of level 2 and 3 of digestion, meaning that digestion had started, but one could still separate systematic groups, and possibly identify species (which was not attempted in this thesis). Statistical tests did not show any significant differences between night and day for the level of filling ($p > .05$) of neither species, nor for level of digestion for *M. muelleri*. However, the tests did show a significant difference between night and day for level of digestion for *B. glaciale* ($p << .05$) with content from stomachs sampled at night time being more digested than those sampled at daytime.

3.5 Vertical distribution of zooplankton from the MOCNESS

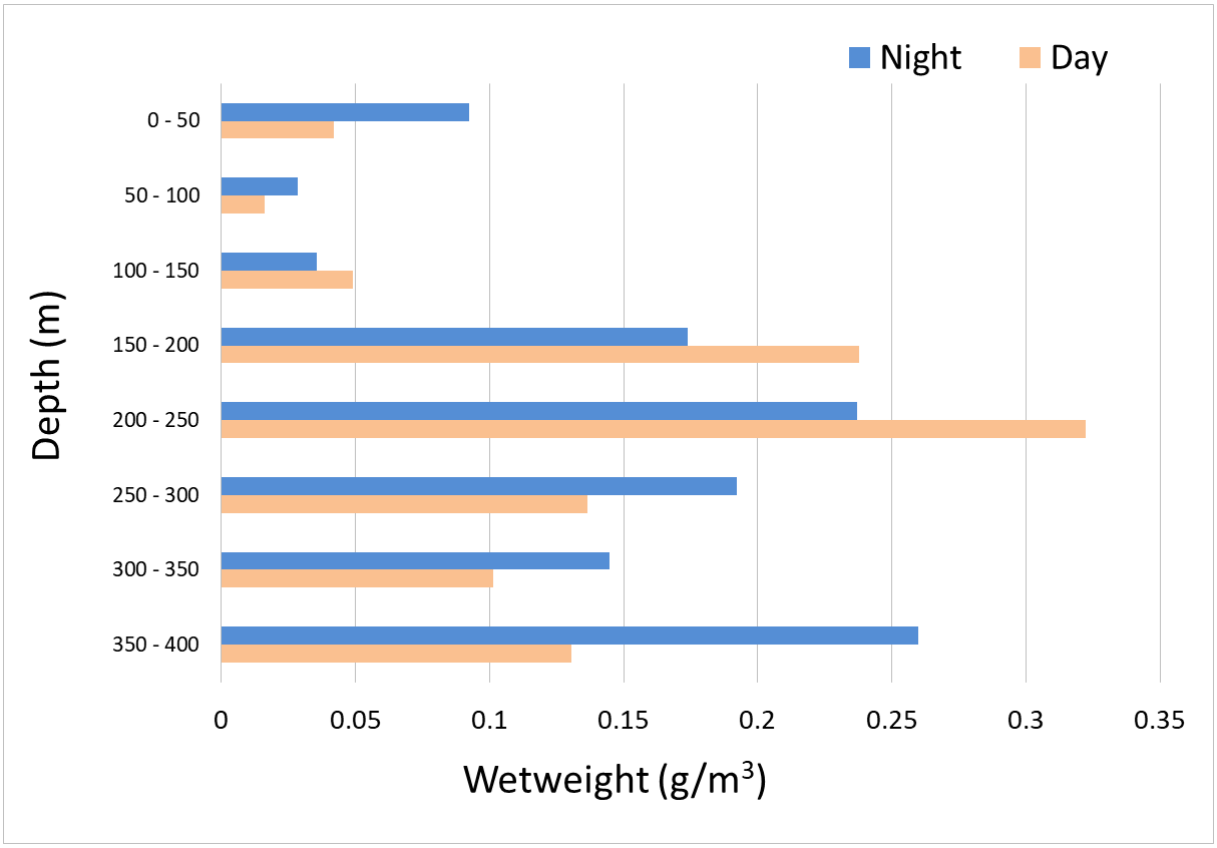

Figure 9. Distribution in the water column of the total weight of zooplankton caught at night and day.

The vertical distribution of zooplankton, measured in g/m^3, revealed considerably higher values for the water masses below ~150 m, than for the upper 150 m, for both day and night (Figure 9). The distribution of the daytime catches peak at 200 - 250 m, while the distribution for the night time catches show the highest numbers at 350 - 400 m.

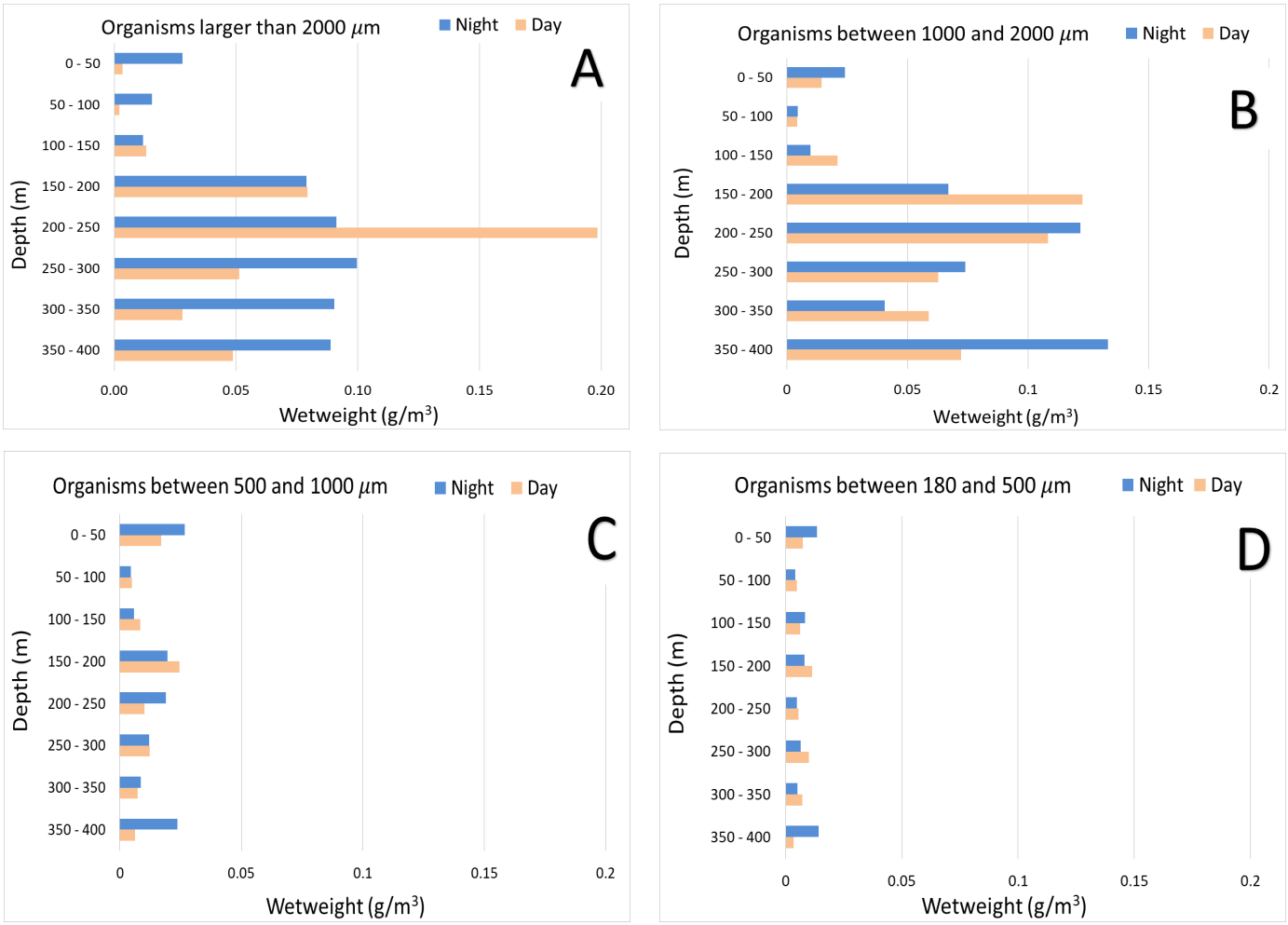

Figure 10. Distribution of different size groups of zooplankton in the water column. Organisms larger than 2000µm (A), organisms between 1000 and 2000 µm (B), organisms between 500 and 1000 µm (C) and organisms between 180 and 500 µm (D)

The water column is dominated (in means of biomass) by organisms > 1000 µm (Figure 10). Most of the organisms larger than 2000 µm are found at the depths from 150 - 400 m, with and obvious daytime peak at 200 - 250 m, and with the night time catches distributed rather evenly from 150 - 400 m (Figure 10A). Organisms between 1000 - 2000 µm are also mainly distributed deeper than 150 m (Figure 10B). Organisms between 500 - 1000 µm seem to have a polymodal distribution from the night time catches with main peaks at 0 - 50 m, 150 - 250 m and 350 - 400 m. The daytime catches from the same size group peak at 0 - 50 m and 150 - 200 m (Figure 10C). Night time catches for organisms between 180 - 500 µm have two obvious peaks at 0 - 50 m and 350 - 400 m. The peak for the day time catch is found at 150 - 200 m (Figure 10D).

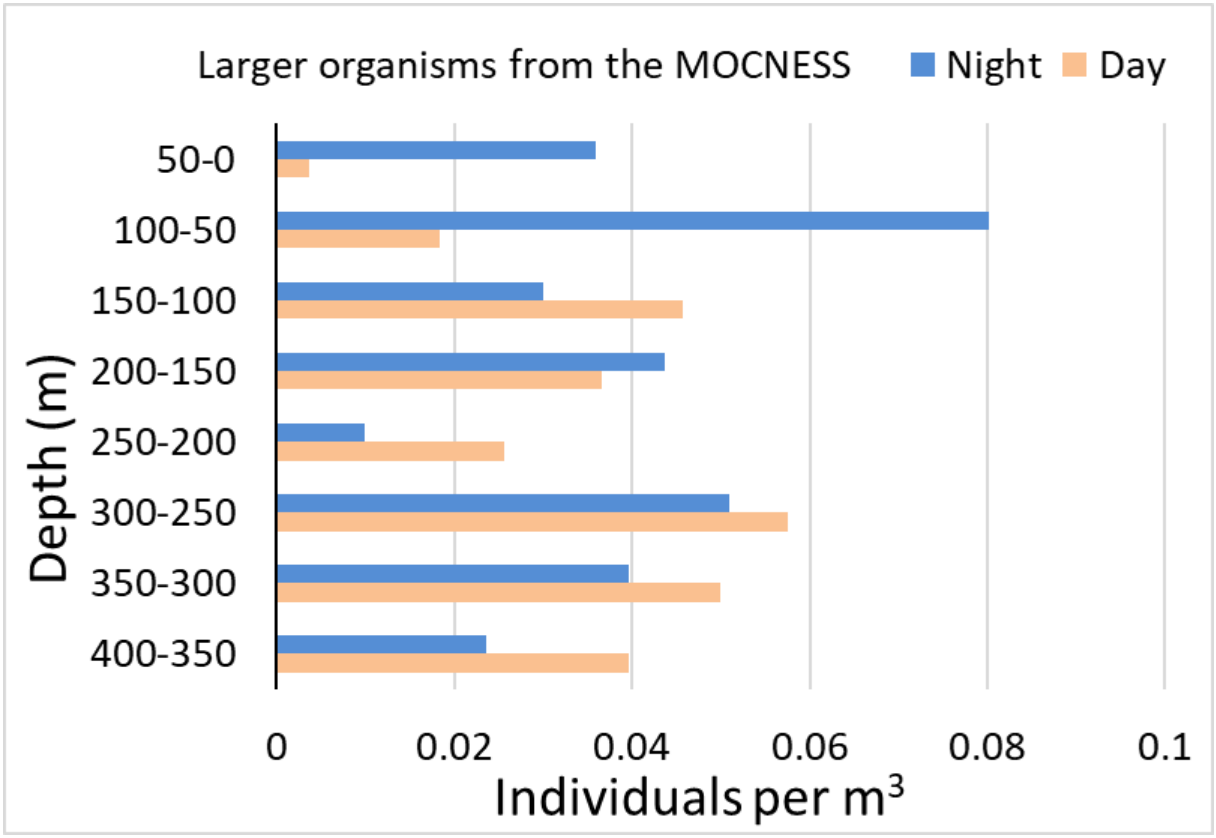

Figure 11. Larger organisms from the MOCNESS caught at night and day.

Larger organisms such as krill, shrimps and individuals of *B. glaciale* and *M. muelleri* were picket out from the MOCNESS cups, counted and identified, before the remaining catch was put on formalin. These species/organisms are therefore not a part of the size distributions shown in Figure 10, (though they belong to the group > 2000 µm).

The major proportion of the larger organisms caught and counted from the MOCNESS was krill (*Meganyctiphanes norvegica* and *Nematoscelis sp., og arctica*) and shrimps (*Boreomysis arctica*, *Pasiphea sp.* and *Sergestes sp.*). The night time distribution is clearly densest at 50 - 100 m, with a value of 0.08 individuals per m^3 (Figure 11). The daytime distribution is more even, with two peaks at 100 - 150 m (0.046 ind/m^3) and 250 - 300 m (0.058 ind/m^3) (Figure 11). The least abundant depth interval is 0 - 50 m (0.0037 ind/m^3) from the day time catch, and 200 - 250 m (0.099 ind/m^3) from the night time catch.

3.6 Acoustic data

3.6.1 Echogram of the water column from the 15th to the 21st of November (2015)

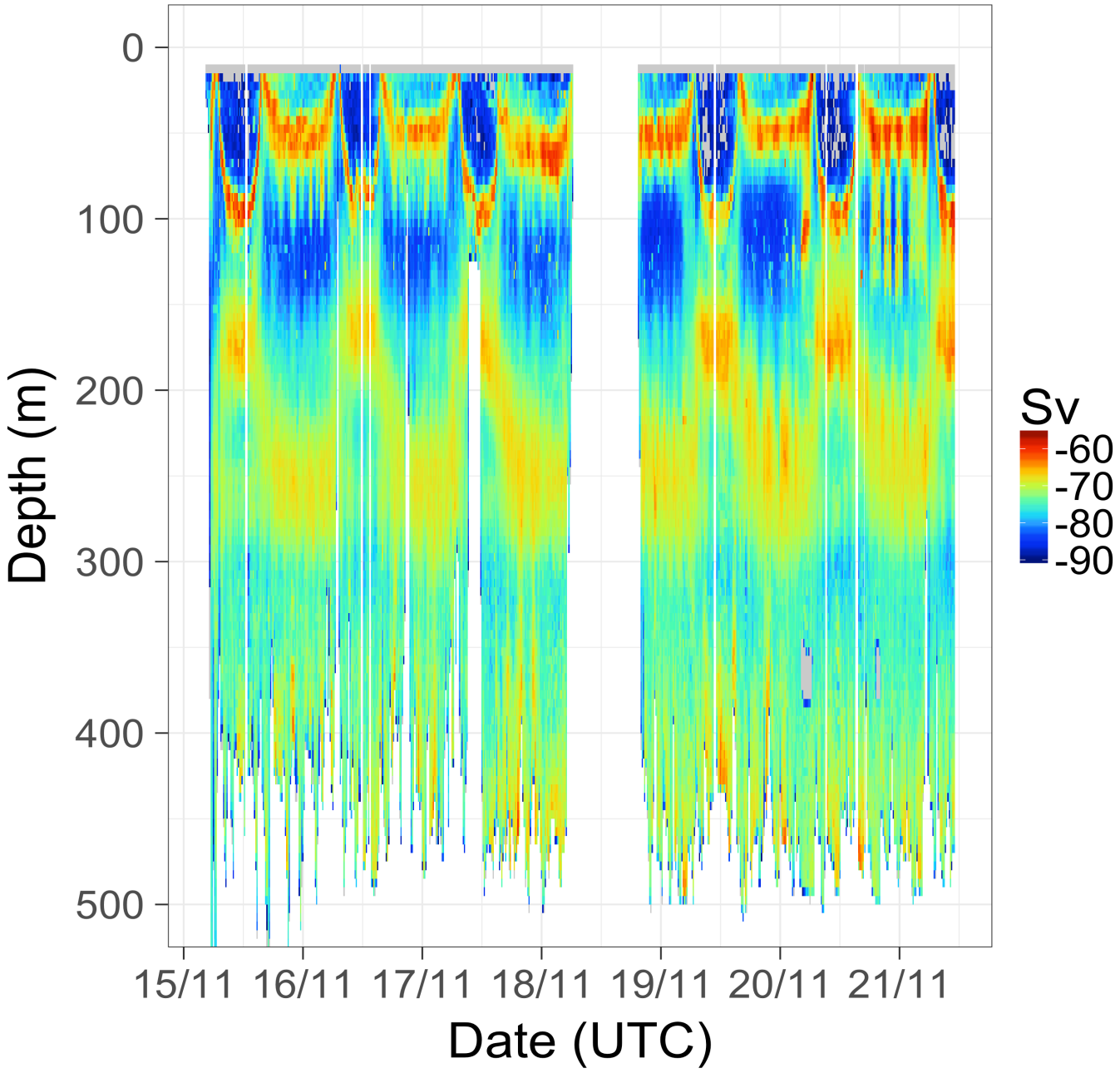

Figure 12. "The vertical distribution of the mesopelagic scattering layer given as the (mean) volume backscattering strength, Sv (dB re 1 m^{-1}), as a function of date where UTC is used for time."

Two distinct backscattering layers are seen in the echogram (Figure 12), from now on referred to as SSL1 and SSL2. The daytime depth of SSL1 is approximately 100 m. At dusk the SSL1 migrates to the surface, with a subsequent descend to around 50 m at midnight, before

migrating to the surface again at dawn and then migrating back to the deeper daytime distribution. SSL2 has a daytime distribution at approximately 150 m. At dusk the SSL2 descends to deeper waters, being distributed between 270 to 300 m, before migrating back to the shallower daytime distribution at dawn. The daytime distribution for the SSL2 is denser than the night time distribution, which is more dispersed. There also seem to be some overlap between the two layers at daytime.

3.6.2 Echogram of the water column (24 h) with simultaneous surface irradiance

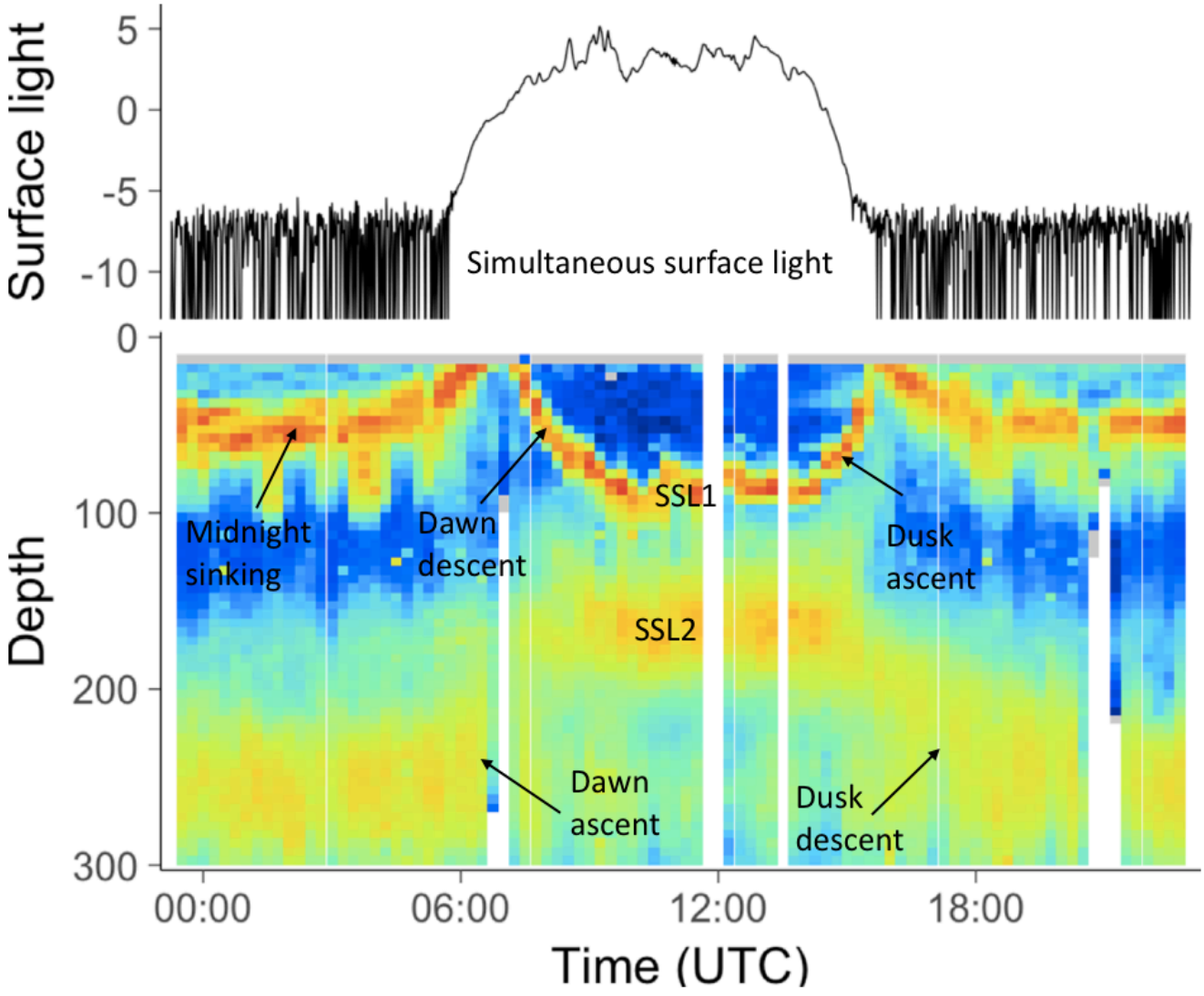

Figure 13. The two mesopelagic sound scattering layers on the 16th of November (bottom) collated with simultaneous measurements of surface irradiance (top). Light intensities below a value of 10^{-5} is below the sensitivity of the radiometer and is present as noise in the figure.

Figure 13 shows the 24 h distribution of SSL1 and SSL2 compared to the concurrent surface illumination from the 16th of November (2015). There is some overlap between the two backscattering layers at daytime, as SSL1 is distributed at its deepest and SSL2 at its shallowest. SSL1 has a narrower and denser distribution than SSL2. The daytime distributions of both layers seem to continuously change their position in relation to variation in surface light (i.e cloud cover and sun position), instead of remaining at a constant daytime depth.

3.6.3 Averaged volume backscatter in the watercolumn

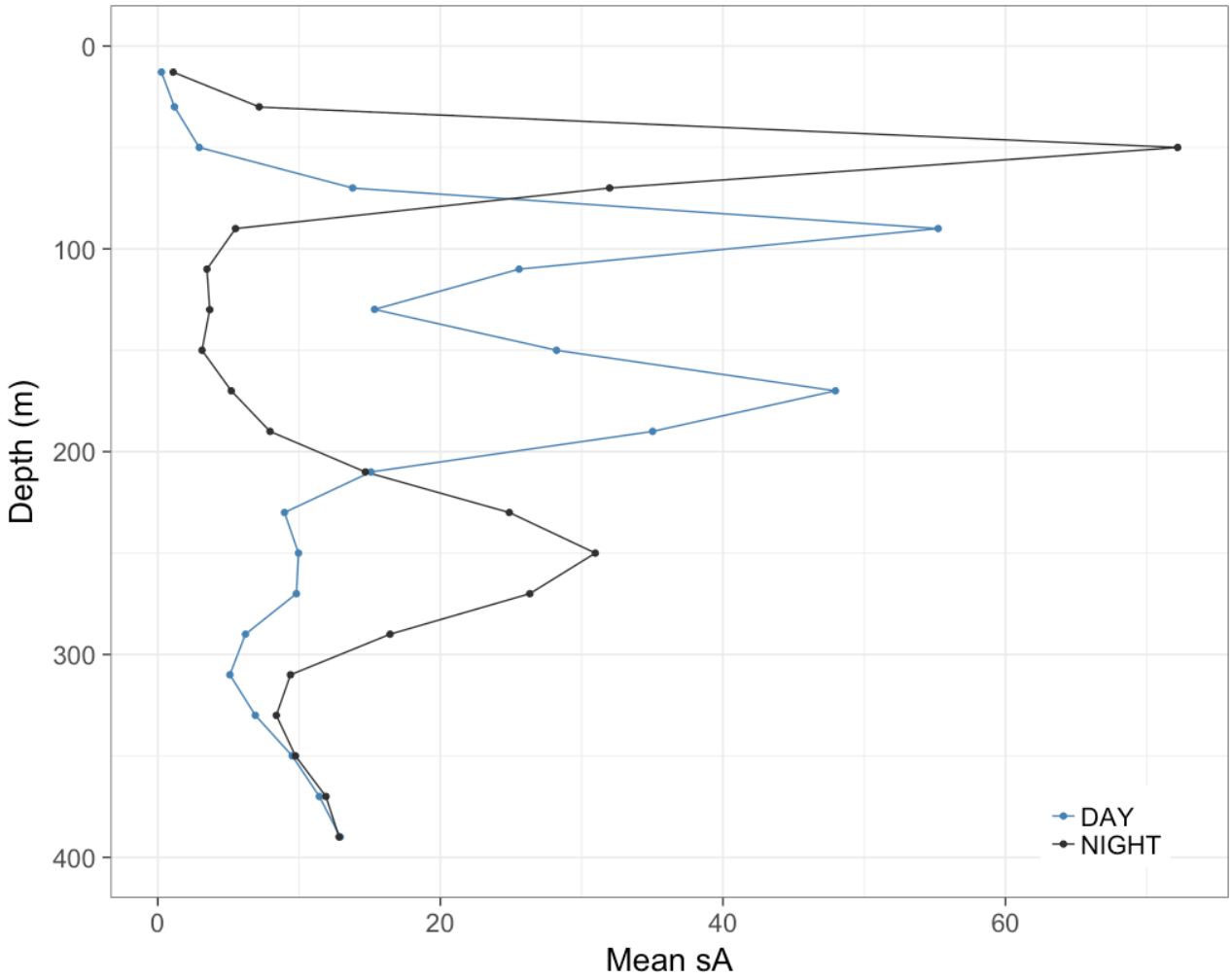

Figure 14 Mean S_A (Nautical area scattering strength (dB re 1 (m^2 nmi^{-2}))), plotted against depth (m). Mediated at every 20m depth, between 10-14 for day and 22-02 for night, for the whole period (15.11-21.11).

Volume backscatter is averaged for 20 m intervals for day (10-14) and night (22-02) for the period of 15th – 21st of November. Two peaks are present at both night and day. The shallowest peak (both night and day) represent SSL1, while the deepest represent SSL2. The scattering strength (Mean S_A) is highest for the nighttime layer of SSL1.

3.7 Estimated irradiance at daytime SSL depths

Table 4. Estimated irradiance (mW m^{-2} $nm^{-}1$) at 485 nm at daytime SSL depths at the 16th of November. Time in UTC.

SSL1		SSL2	
Depth (m)	Daytime (12:00)	Depth (m)	Daytime (12:00)
80	1.32E-03	150	1.07E-05
81	1.23E-03	151	9.96E-06
82	1.15E-03	152	9.29E-06
83	1.07E-03	153	8.68E-06
84	1.00E-03	154	8.10E-06
85	9.37E-04	155	7.56E-06
86	8.74E-04	156	7.06E-06
87	8.16E-04	157	6.59E-06
88	7.62E-04	158	6.15E-06
89	7.11E-04	159	5.74E-06
90	6.64E-04	160	5.36E-06
91	6.20E-04	161	5.00E-06
92	5.78E-04	162	4.67E-06
93	5.40E-04	163	4.36E-06
94	5.04E-04	164	4.07E-06
95	4.71E-04	165	3.80E-06
96	4.39E-04	166	3.54E-06
97	4.10E-04	167	3.31E-06
98	3.38E-04	168	3.09E-06
99	3.57E-04	169	2.88E-06
100	3.33E-04	170	2.69E-06
		171	2.51E-06
		172	2.35E-06
		173	2.19E-06
		174	2.04E-06
		175	1.91E-06
		176	1.78E-06
		177	1.66E-06
		178	1.55E-06
		179	1.45E-06
		180	1.35E-06

Table 5. Estimated ambient irradiance (mW m^{-2} $nm^{-}1$) at 485nm at 06:00 (UTC). Estimated with a surface irradiance of 1×10^{-05} mW m^{-2} $nm^{-}1$,

Depth (m)	Ambient irradiance at 06:00
20	2.13E-07
250	7.12E-15

Table 4 shows the daytime irradiance at depth estimated from the surface irradiance at the 16th of November 12:00 (UTC). The SSL1 is distributed from about 80 to100 m at daytime, and the SSL2 from about 150 m to 180 m. The estimated light values in this table is equivalent to the estimated light comfort zones (LCZ) of the SSLs. The daytime mean S_A peak for the SSL1 (~90 m) and the SSL2 (~170 m) (Figure 14) corresponds to the estimated light values of 6.64×10^{-4} and 2.69×10^{-6} (Table 4). SSL1 and SSL2 thus have different LCZ with light intensities differing approximately two orders of magnitude.

Table 5 shows the ambient irradiance (485 nm) at the mean depth distribution at 06:00 for the SSL1 (20 m) and SSL2 (250 m) (Figure 13). The ambient irradiances are estimated from a surface irradiance of 1×10^{-05} mW m^{-2} $nm^{-}1$. The ambient irradiances for the two SSLs at 06:00 (UTC) differ eight orders of magnitude.

4. DISCUSSION

The acoustic data presented in the echogram shows two sound scattering layers with distinct diel migration patterns. The shallowest layer (SSL1) displays a daytime distribution at ~ 100 m, ascending to the surface at dusk, followed by a subsequent midnight sinking to ~ 50 m, ascending to the surface at dawn, before migrating back to its daytime distribution. The deeper layer exhibiting inverse diel vertical migration (SSL2) has its shallowest distribution at daytime, ~170 m, and migrates to deeper waters at night, ~250 m. The daytime distribution is more confined than the deeper night time distribution. These patterns will be discussed in relation to hydrography, surface irradiance, estimated ambient light in the water column, vertical distribution of zooplankton biomass, length distribution and stomach analysis of the two mesopelagic fish species *B. glaciale* and *M. muelleri*.

The composition of the two sound scattering layers (SSL1 & SSL2) visible in the echogram cannot, with certainty, be established from the observations in Bjørnafjorden. Both the mesopelagic fish species *M. muelleri* and *B. glaciale* were present in virtually all hauls. The sampling could not confirm whether these species constituted either of the two layers. Trawling at specific depth intervals could have given valuable information about the vertical position of these species, but unfortunately no such hauls were taken during this cruise. Still, previous studies from the nearby Norwegian fjord *Masfjorden* conducted such hauls. The results have shown that *M. muelleri* is the prevailing species linked to the acoustic backscatter in the upper ~ 200 m of the water column (Giske et al., 1990, Staby and Aksnes, 2011), while *B. glaciale* dominates the scattering layers below ~ 200 m (Kaartvedt et al., 1988, Bagøien et al., 2001, Dypvik et al., 2012b). This leads to the assumption that *M. muelleri* and *B. glaciale* also here constitutes the main body of SSL1 and SSL2, accordingly. This assumption is further supported by previous studies ascribing these species to scattering layers with similar migration patterns as those observed in Bjørnafjorden (Giske et al., 1990, Kaartvedt et al., 2009, Dypvik et al., 2012a).

4.1 Length distributions of *B. glaciale* and *M. muelleri*

The results from the length measurements revealed two distinct length groups for *M. muelleri* and three for *B. glaciale.* Correlations between age and length-frequencies has previously been confirmed by comparing analysis of otoliths (Gjøsæter, 1973a, Halliday, 1970). Length groups found in this study can roughly be divided into 14-30 mm, 39-55 mm and > 55 mm, for *B. glaciale*, corresponding to age group 0, age group 1, and age group 2 and older (Gjøsæter, 1973a, Halliday, 1970). For *M. muelleri*, the length groups can be divided into 11-20 mm and 33-53 mm, equivalent to age group 0 and age group 1, accordingly. The few specimens of *M. muelleri* that measured > 53 mm, is believed to be age group 2 or older. Age group 0 refers to the individuals that were hatched the preceding spring and are not yet mature.

Previous studies from Masfjorden have observed that different age groups differ in their behavioral strategies in terms of varying diel vertical migration patterns (Giske et al., 1990, Kaartvedt et al., 2009, Dypvik et al., 2012b). Juveniles of *M. muelleri* has been observed to carry out vertical migrations with midnight sinking, while adult *M. muelleri* stayed in a deeper layer with more restricted migrations at dusk and dawn, or with no migration at all (Giske et al., 1990, Dypvik et al., 2012a). Several migration strategies have also been found for *B. glaciale.* Dypvik et al. (2012a) found two backscatter layers below ~200 m. One layer exhibiting IDVM, and one layer that stayed at depth, not migrating at all. The fish constituting these two deep layers were of the two largest size groups, while the smallest size group were distributed shallower, overlapping with the pearlsides.

Trawl hauls were done through the whole water column, and no sampling at specific depth intervals were done (except from with the MOCNESS). The two MOCNESS hauls described in this thesis contained 7 specimens of *B. glaciale* and 2 specimens of *M. muelleri* all together, too few to make any conclusions about their vertical distribution. Ascribing different age groups to the backscattering layers can therefore not be done, but expectations can be made based on findings from previous studies, as mentioned initially (Giske et al., 1990, Kaartvedt et al., 2009, Dypvik et al., 2012a). The SSL1 exhibiting midnight sinking is most likely age group 0 of *Maurolicus muelleri*, while the deeper SSL2 is most likely age group 1 and older individuals of *Benthosema glaciale.* This would be in accordance with Heinckes law that the average size of the individuals increases with depth (Linehan et al., 2001).

Although the other age groups from both species were present in the water column, they could not be detected in the echogram. Possible reasons for this could be that they did not form aggregations dense enough to be detected by the echosounder or that they may have been distributed together with the SSL1 and SSL2.

4.2 Hydrographic properties of the water column in relation to the SSLs

A study by Bianchi et al. (2013) showed oxygen concentrations to be the most important single predictor for migration depths on a global scale. In general, regions with higher subsurface oxygen concentrations were correlated to deeper migration depths, while areas with low oxygen concentrations were correlated with shallower migration depths. Klevjer et al. (2016) further stated that oxygen levels could be linked to the proportion of migrating individuals in a scattering layer. Both studies report findings on a global scale, with high variations in oxygen, ranging from well oxygenated to hypoxic and even anoxic areas. The results from Bjørnafjorden in the present study show a well oxygenated water column, suggesting that the migration patterns and migration depths observed here are not effected by oxygen concentrations. The somewhat lower oxygen concentration at ~50 m can most likely be explained by high respiration rates at this depth, possibly from the SSL1.

Salinity ranged from 30 to 34 PSU from the surface to approximately 70 m. This is characteristic for the Norwegian Coastal Water (NCW, PSU < 34.5). Runoffs from rivers into the fjord might also contribute to a less saline surface. The salinity concentrations were stable below the depth of ~150 m (35.25 PSU). This concentration is characteristic for water masses from the North Atlantic Water (NAW, PSU > 35.). To my knowledge salinity concentration has not previously been linked to DVM or migration depths.

There was a temperature maximum at 12°C between 25 to 50 m, overlapping the night time distribution of the SSL1. A study by Wurtsbaugh and Neverman (1988) suggested that fish migrate to warmer waters after feeding to increase their digestion rate, and thereby growth. The possible importance of this finding will be discussed later. Studies by Sameoto (1989) and Halliday (1970) have shown that *B. glaciale* can tolerate temperatures down to 0° C and up to 18° C, but prefer temperatures between 3° to 12°C. The SSL2 (the inverse migrating

layer) was always distributed deeper than ~150 m, where the temperatures were stable at ~7.5° C. This suggests that temperature did not affect the migration pattern, nor the migration amplitude for the SSL2.

4.3 Light in relation to the SSLs

Surface irradiance was continuously measured during the whole cruise. The radiometer was not sensitive enough to measure nighttime irradiance. Autumn and winter in Norway is characterized by long nights and short days, and valid light measurements could be obtained from around ~06-07:00 to ~16:00. At midday, when light intensities were at its strongest, SSL1 was distributed at its deepest (~100 m) and SSL2 at its shallowest (~175 m). When light intensities decreased at dusk, SSL1 migrated to the surface. This appears consistent with SSL1 staying within a LCZ (Staby and Aksnes, 2011, Røstad et al., 2016). In addition to the extensive migrations at dusk and dawn, the scattering layers also seemed to adjust their daytime distribution in accordance to changes in incoming surface light, such as varying cloud cover and sun position (Figure 13). Instead of being distributed at a fixed depth, the SSL1 made instantaneous changes, ascending or descending a few meters to correct for the changes in ambient light levels. This is in accordance with previous studies (Giske et al., 1990, Baliño and Aksnes, 1993, Rasmussen and Giske, 1994). The observations made at daytime when surface light was sufficiently high to be measured further supports the hypothesis of a LCZ (Dupont et al., 2009, Røstad et al., 2016).

The attenuation coefficients for downwelling irradiance (K) in Bjørnafjorden were estimated from the two underwater measurements conducted on the 15th and the 19th of November. These estimates revealed that light was attenuated faster in the upper part of the water column than it was in the deeper water masses. These results are consistent with the findings of Norheim et al. (2016), where the attenuation slope of the water column grouped into two layers with separate attenuation coefficients. The estimated light intensities at depth gives a clear indication of different LCZ for the two layers (Table 4). Sensitivity to light vary between species (Warrant and Adam Locket, 2004, de Busserolles et al., 2017) and it seems like the *B. glaciale* is better adapted to lower light intensities than *M. muelleri*. Difference in

depth distributions may also be modified by size and ontogenetic stages within the species (Goodson et al., 1995, Staby et al., 2011).

Ambient irradiance at midday were estimated for the depth range of the two scattering layers, SSL1 and SSL2 (Table 4). Both scattering layers were distributed in depths where light intensities spanned over an order of magnitude. The light levels of the SSL1 spanned from 1.3 $\times 10^{-3}$ to 3.3 $\times 10^{-4}$ mW m^{-2} nm^{-1}, while the levels of SSL2 spanned from 1.1 $\times 10^{-5}$ to 1.4 $\times 10^{-6}$ mW m^{-2} nm^{-1}. The light intensities where the two layers were densest, ~90 m for SSL1 and ~170 m for SSL2 (Figure 14), were 6.6 $\times 10^{-4}$ mW m^{-2} nm^{-1} and 2.7 $\times 10^{-6}$ mW m^{-2} nm^{-1}, accordingly. Hence, the preferred light intensities for the SSL2 was about two orders of magnitude lower than for the SSL1. The estimated light intensities for the SSL2 in Bjørnafjorden match those found in a previous study. Norheim et al. (2016) found the ambient irradiance of the mean depth of the SSL in their study to be 2 $\times 10^{-6}$ mW m^{-2} nm^{-1}. Their cruise was conducted during summer, with relatively high light intensities even during the night. They found that the scattering layer kept the ambient irradiance within the LCZ through the day and night, by migrating to shallower waters at dusk, and back in the depth at dawn. The study in Bjørnafjorden were however conducted during the late fall, and the surface light at night might here have been too low to provide LCZs for SSL1 and SSL2 during night time. Anyway, other factors than light must have been responsible for the deepening of SSL1 and SSL2 at night.

4.5 Possible explanations for midnight sinking of the SSL1

The findings in this study revealed a distinct pattern of midnight sinking for the shallow scattering layer (SSL1), with a nocturnal distribution between ~ 30 to 70 m (Figure 12) and peak mean S_A (Nautical area scattering strength) at 50 m (Figure 14). This migration pattern has previously been reported for the lanternfish *M.muelleri* (Giske et al., 1990), and recent studies put this pattern in a seasonal context, occurring in autumn and ceasing in spring (Staby et al., 2011, Prihartato et al., 2015). This seasonal cycle seems to be correlated to the change in incoming surface irradiance through the year, at high latitudes. Both Staby et al. (2011) and Prihartato et al. (2015) reported that the pattern of midnight sinking was initiated when light levels started to drop in autumn and ceased in the spring when light levels increased again,

but without being able to refer to specific levels of light due to lack of instrumental sensitivity.

M. muelleri have eyes adapted for foraging in relatively bright light in the upper part of the mesopelagic environment, within a certain range of light levels (de Busserolles et al., 2017). They are known to momentarily change their vertical position in the water column, to keep within their preferred range of light levels, the light comfort zone (LCZ) (Giske et al., 1990, Baliño and Aksnes, 1993, Rasmussen and Giske, 1994). Results from the present study revealed a LCZ for *M. muelleri* (SSL1) with underwater light intensities (485 nm) spanning from 1.32×10^{-3} to 3.33×10^{-4} mW m^{-2} nm^{-1} (Table 4), almost one order of magnitude. These underwater light values are estimated based from surface irradiance at midday (16^{th} of November) and corresponds to depths from 80 to 100 m. Following the predictions of the LCZ, the individuals of the scattering layer will be expected to constantly keep within this LCZ. When the ambient light in the epipelagic fall below this LCZ, however, it might be hypothesized that light can no longer be used as a point of reference in regards of depth distributions.

Due to lack of sensitivity in the radiometer surface irradiance could not be measure during the dark November nights (16^{th} - 20^{th}) in the present investigation. The ambient light exposure at nighttime of the SSLs could therefore not be determined. Nevertheless, some estimates based on the measurements considered valid can be made. The individuals of the SSL1 started their morning ascend around 05:00 (UTC) (Figure 13), ascending from their midnight sinking depth to the surface. At this time, the radiometer was still not sensitive enough to measure incoming surface irradiance. The radiometer can measure light intensities (485 nm) down to approximately 10^{-5} mW m^{-2} nm^{-1}. These intensities could be measured from around 06:00 (UTC). Estimates based on the surface irradiance and the depth of the SSL1 at 06:00 (~ 20 m) revealed ambient light intensities (485 nm) at 2.1×10^{-7} mW m^{-2} nm^{-1}. *M. muelleri* thus responds to changes in light when the ambient light intensities (485 nm) > 2.1×10^{-7} mW m^{-2} nm^{-1}. Even though it cannot be verified due to lack of data, it is highly likely that *M. muelleri* also reacts to light intensities below this, as they started their migration about an hour before surface irradiance could be measured.

If light intensities of the water column fell below the LCZ, other factors than light might explain the the midnight sinking and depth distributions of the scattering layers at night.

Wurtsbaugh and Neverman (1988) studied migration patterns of fish in a lake and suggested that they migrate to warmer water masses after feeding, as a strategy for stimulating digestion, leading to greater feeding and growth. My results reveal that the night time depth distribution of SSL1 at 50 m does indeed overlap with the temperature maximum (12°C) of the water column, 2 degrees warmer than the surface layer and 4.5 degrees warmer than the stable layer below 150 m. Giske et al. (1990) observed the same overlap, but still rejected this suggestion. They found that the fish in their research had no food intake at night, proposing that migrating to warmer water would only lead to a net cost of respiration. In the present study samples of *M. muelleri* were dominated by intermediate levels of stomach filling and did not show any significant differences in level of stomach filling between night and day (Figure 8). Midnight sinking as a strategy for stimulating digestion can therefore not be rejected based on my data.

Staby et al. (2011) studied the migration pattern of *M. muelleri* over a period of 15 months, and found that temperature profiles could not be linked to the nocturnal depth distribution. Instead they hypothesized that the fish migrate to deeper waters to avoid the predators foraging in shallow waters. Predator data was not a part of the present investigation in Bjørnafjorden, so the hypothesis cannot be rejected nor supported. Speculations could be made that in the absence of light the fish swim randomly. Expectations would then be a more dispersed scattering layer with individuals distributed both deeper and shallower. This is contradicted by the dense aggregations formed by the scattering layer.

4.6 Possible explanations for the IDVM of the SSL2

The deepest scattering layer (SSL2) detectable in the echogram exhibited a patterns of inverse diel vertical migration (IDVM), ascending to a daytime depth between ~150-200 m, and descending to deeper layers at dusk. The pattern of inverse diel vertical migration has previously been described for zooplankton (Ohman et al., 1983), but not until recently for mesopelagic fish. Ohman et al. (1983) studied the inverse DVM patterns of the copepod *Pseudocalanus* sp. and noted that these migrations concurred with the normal DVM of tactile invertebrate predators. Observations revealed that this reduction in spatial overlap seemed to decrease the mortality rate of adult females of the *Pseudocalanus* sp. This explanation does

not necessarily apply to the IDVM of mesopelagic fish as their main predators are visual foragers and does not exhibit patterns of DVM.

Kaartvedt et al. (2009) studied the migration patterns of mesopelagic sound scattering layers in Masfjorden, west in Norway, and found that one of the scattering layers attributed to *B. glaciale* carried out inverse DVM during autumn. They suggested that this behavior could be explained as individuals seeking better light conditions in daytime, to be able to visually forage on overwintering *Calanus*, before returning to deeper waters at night. The same pattern of IDVM was found by Dypvik et al. (2012a) the following year. These studies, however, did not contain any simultaneous light measurements. They were therefore not able to confirm whether the depth *B. glaciale* migrated to at daytime contained enough light for visual detection of prey.

In the present study, a LCZ of *B. glaciale* was estimated, i.e the estimated irradiance corresponding to the daytime depth of the SSL2. The findings here (Table 4) supports the theory of *B. glaciale* migrating to depths with better light conditions at daytime, possibly to feed (Kaartvedt et al., 2009, Dypvik et al., 2012a). The maximum S_A (Nautical area scattering strength) for the SSL2 in Bjørnafjorden had a daytime depth at ~ 170 m and an estimated light level of 2.7×10^{-6} mW m^{-2} nm^{-1}. These light intensities are equivalent to the LCZ described by Norheim et al. (2016) for a scattering layer in the Norwegian Sea.

During daytime, when surface light could be measured, *B. glaciale* seemed to follow a preferred LCZ using light as a point of reference, responding to light intensities within a certain range. The results in this thesis (Figure 13) revealed that the individuals of the SSL2 starts their morning ascend around 06:00, and that this correspond to when the surface light just exceed the light intensities of 10^{-5} mW m^{-2} nm^{-1}. Estimates of the ambient irradiance at the mean depth of the SSL2 at 06:00 (~250 m) reveal a light intensity (485 nm) of 7.1×10^{-15} mW m^{-2} nm^{-1}. *B. glaciale* thus seem to respond to changes in light when the ambient light intensities (485 nm) exceed 7.1×10^{-15} mW m^{-2} nm^{-1}. Unfortunately, the radiometer was not sensitive enough to measure surface light below a threshold of approximately 10^{-5} mW m^{-2} nm^{-1} (485 nm). The possibility that *B. glaciale* responds to even lower light intensities cannot be excluded.

The investigations of Kaartvedt et al. (2009) and Dypvik et al. (2012a) revealed that the individuals with IVDM in Masfjorden seemed to mainly feed during daytime, and that their stomach content were dominated by copepods of the genus *Calanus*. Stomach content were not attempted identified in this study from Bjørnafjorden, but previous studies show *Calanus* to be an important part of the diet of *B. glaciale* (Sameoto, 1988, Bagøien et al., 2001, Baliño and Aksnes, 1993). Stomachs from *B. glaciale* from Bjørnafjorden were analyzed based on level of filling and degree of digestion in individuals sampled at day and night. Levels of filling were more or less equal for night and day, while levels of digestion revealed a significant difference between night and day ($p << .05$). The stomach content was more digested in the stomachs sampled at night than those sampled at day.

The digestion time for *B. glaciale* and other mesopelagic fish is not well known, but it is reasonable to assume that low levels of digestion indicate a short time since feeding (Dalpadado and Gjøsæter, 1988, Dypvik et al., 2012a), and that time since feeding increase with the levels of digestion. It is therefore reasonable to believe that the main feeding period for *B. glaciale* in Bjørnafjorden is during the daytime in illuminated waters. These results further support the hypothesis of Kaartvedt et al. (2009) and Dypvik et al. (2012a). Even though results indicate a main feeding period at daytime, feeding during the nighttime using other strategies than vision to detect prey, cannot be excluded. This can still be expected to be somewhat less efficient than visual foraging.

Results from the MOCNESS revealed that the zooplankton biomass was mainly distributed underneath ~150 m, and that the organisms larger than 1000 µm dominated the water column. This is in accordance with previous reported seasonal variations in vertical distribution of zooplankton. Samples from the MOCNESS were not identified by species or genus, but previous observations report that from autumn to spring, the major proportion of zooplankton is located beneath 150 m (Giske et al., 1990, Bagøien et al., 2001, Baliño and Aksnes, 1993). Several species of the *Calanus* copepod, which is known to be the preferred prey for *B. glaciale* in Norwegian fjords (Gjøsæter, 1973b), are known to carry out seasonal migrations during autumn, descending to midwaters, entering an inactive state of overwintering (Hirche, 1996, Bagøien et al., 2001). This might help explain why individuals of *B. glaciale* does not ascend to the surface at dusk. When prey abundance is sufficient, and even greater, in the depths below ~150 m, than for the surface layer, there will be no further motivation for migrating to the surface for foraging.

To my knowledge none of the hypothesis attempting to explain IDVM in *B. glaciale* have suggested factors governing their night time distribution. Although this *B. glaciale* is mainly considered a visual feeder it cannot be excluded that *B. glaciale* also feed in the dark, using other strategies than vision to detect prey. In that case, if sight is no longer an option, migrating to the highest concentration of prey would be profitable. A hypothesis may therefore be that when light intensities fall outside the LCZ of *B. glaciale*, they distribute according to the highest concentration of prey in the water column. This will need to be further investigated.

5. LITERATURE CITED

AKSNES, D. L., RØSTAD, A., KAARTVEDT, S., MARTINEZ, U., DUARTE, C. M. & IRIGOIEN, X. 2017. Light penetration structures the deep acoustic scattering layers in the global ocean. *Science advances,* 3**,** e1602468.

BAGØIEN, E., KAARTVEDT, S., AKSNES, D. L. & EIANE, K. 2001. Vertical distribution and mortality of overwintering Calanus. *Limnology and Oceanography,* 46**,** 1494-1510.

BALIÑO, B. M. & AKSNES, D. L. 1993. Winter distribution and migration of the sound scattering layers, zooplankton and micronekton in Masfjorden, western Norway. *Marine Ecology-Progress Series,* 102**,** 35-35.

BENNETT, W. A., KIMMERER, W. J. & BURAU, J. R. 2002. Plasticity in vertical migration by native and exotic estuarine fishes in a dynamic low‐salinity zone. *Limnology and Oceanography,* 47**,** 1496-1507.

BIANCHI, D., GALBRAITH, E. D., CAROZZA, D. A., MISLAN, K. A. S. & STOCK, C. A. 2013. Intensification of open-ocean oxygen depletion by vertically migrating animals. *Nature Geoscience,* 6**,** 545.

BUESSELER, K. O. & BOYD, P. W. 2009. Shedding light on processes that control particle export and flux attenuation in the twilight zone of the open ocean. *Limnology and Oceanography,* 54**,** 1210-1232.

CLARK, C. W. & LEVY, D. A. 1988. Diel Vertical Migrations by Juvenile Sockeye Salmon and the Antipredation Window. *The American Naturalist,* 131**,** 271-290.

DALPADADO, P. & GJØSÆTER, J. 1988. Feeding ecology of the lanternfish Benthosema pterotum from the Indian Ocean. *Marine Biology,* 99**,** 555-567.

DE BUSSEROLLES, F., CORTESI, F., HELVIK, J. V., DAVIES, W. I., TEMPLIN, R. M., SULLIVAN, R. K., MICHELL, C. T., MOUNTFORD, J. K., COLLIN, S. P. & IRIGOIEN, X. 2017. Pushing the limits of photoreception in twilight conditions: The rod-like cone retina of the deep-sea pearlsides. *Science advances,* 3**,** eaao4709.

DUPONT, N., KLEVJER, T. A., KAARTVEDT, S. & AKSNESA, D. L. 2009. Diel vertical migration of the deep‐water jellyfish Periphylla periphylla simulated as individual responses to absolute light intensity. *Limnology and Oceanography,* 54**,** 1765-1775.

DYPVIK, E., KLEVJER, T. A. & KAARTVEDT, S. 2012a. Inverse vertical migration and feeding in glacier lanternfish (Benthosema glaciale). *Marine Biology,* 159**,** 443-453.

DYPVIK, E., ROSTAD, A. & KAARTVEDT, S. 2012b. Seasonal variations in vertical migration of glacier lanternfish, Benthosema glaciale. *Marine Biology,* 159**,** 1673-1683.

GISKE, J., AKSNES, D. L., BALIÑO, B. M., KAARTVEDT, S., LIE, U., NORDEIDE, J. T., SALVANES, A. G. V., WAKILI, S. M. & AADNESEN, A. 1990. Vertical distribution and trophic interactions of zooplankton and fish in Masfjorden, Norway. *Sarsia,* 75**,** 65-81.

GJØSÆTER, J. 1973a. AGE, GROWTH, AND MORTALITY OF MYCTOPHID FISH, BENTHOSEMA-GLACIALE (REINHARDT), FROM WESTERN NORWAY. *Sarsia***,** 1-14.

GJØSÆTER, J. 1973b. FOOD OF MYCTOPHID FISH, BENTHOSEMA-GLACIALE (REINHARDT), FROM WESTERN NORWAY. *Sarsia***,** 53-58.

GJØSÆTER, J. 1981. Life history and ecology of Maurolicus muelleri (Gonostomatidae) in Norwegian waters.

GJØSÆTER, J. & KAWAGUCHI, K. 1980. *A review of the world resources of mesopelagic fish*, Food & Agriculture Org.

GOODSON, M., GISKE, J. & ROSLAND, R. 1995. Growth and ovarian development of Maurolicus muelleri during spring. *Marine Biology,* 124**,** 185-195.

HALLIDAY, R. G. 1970. Growth and Vertical Distribution of the Glacier Lanternfish, Benthosema glaciale, in the Northwestern Atlantic. *Journal of the Fisheries Research Board of Canada,* 27**,** 105-116.

HAYS, G. C. A review of the adaptive significance and ecosystem consequences of zooplankton diel vertical migrations. 2003 Dordrecht. Springer Netherlands, 163-170.

HIRCHE, H.-J. 1996. Diapause in the marine copepod, Calanus finmarchicus—a review. *Ophelia,* 44**,** 129-143.

IRIGOIEN, X., KLEVJER, T. A., RØSTAD, A., MARTINEZ, U., BOYRA, G., ACUÑA, J., BODE, A., ECHEVARRIA, F., GONZÁLEZ-GORDILLO, J. I. & HERNANDEZ-LEON, S. 2014. Large mesopelagic fishes biomass and trophic efficiency in the open ocean. *Nature communications,* 5**,** ncomms4271.

KAHILAINEN, K. K., MALINEN, T. & LEHTONEN, H. 2009. Polar light regime and piscivory govern diel vertical migrations of planktivorous fish and zooplankton in a subarctic lake. *Ecology of Freshwater Fish,* 18**,** 481-490.

KAMPA, E. M. & BODEN, B. P. 1954. Submarine illumination and the twilight movements of a sonic scattering layer. *Nature,* 174**,** 869.

KLEVJER, T. A., IRIGOIEN, X., RØSTAD, A., FRAILE-NUEZ, E., BENÍTEZ-BARRIOS, V. M. & KAARTVEDT, S. 2016. Large scale patterns in vertical distribution and behaviour of mesopelagic scattering layers. *Scientific reports,* 6**,** 19873.

KAARTVEDT, S., AKSNES, D. L. & AADNESEN, A. 1988. Winter distribution of macroplankton and micronekton in Masfjorden, western Norway. *Marine Ecology Progress Series,* 45**,** 45-55.

KAARTVEDT, S., STABY, A. & AKSNES, D. L. 2012. Efficient trawl avoidance by mesopelagic fishes causes large underestimation of their biomass. *Marine Ecology Progress Series,* 456**,** 1-6.

KAARTVEDT, S., XF, STAD, A., KLEVJER, T. A. & STABY, A. 2009. Use of bottom-mounted echo sounders in exploring behavior of mesopelagic fishes. *Marine Ecology Progress Series,* 395**,** 109-118.

LAM, V. & PAULY, D. 2005. Mapping the global biomass of mesopelagic fishes. *Sea Around Us Project Newsletter*.

LAMPERT, W. 1989. The adaptive significance of diel vertical migration of zooplankton. *Functional Ecology,* 3**,** 21-27.

LAMPERT, W. & SOMMER, U. 2007. *Limnoecology: the ecology of lakes and streams*, Oxford university press.

LINEHAN, J. E., GREGORY, R. S. & SCHNEIDER, D. C. 2001. Predation risk of age-0 cod (Gadus) relative to depth and substrate in coastal waters. *Journal of Experimental Marine Biology and Ecology,* 263**,** 25-44.

MARSHALL, N. B. 1951. Bathypelagic fishes as sound scatterers in the ocean. *Journal of marine research,* 10**,** 1-17.

MERRETT, N. R. & ROE, H. S. J. 1974. Patterns and selectivity in the feeding of certain mesopelagic fishes. *Marine Biology,* 28**,** 115-126.

MOKU, M., KAWAGUCHI, K., WATANABE, H. & OHNO, A. 2000. Feeding habits of three dominant myctophid fishes, Diaphus theta, Stenobrachius leucopsarus and S. nannochir, in the subarctic and transitional waters of the western North Pacific. *Marine Ecology Progress Series,* 207**,** 129-140.

MOSER, H. G. & AHLSTROM, E. H. The Role of Larval Stages in Systematic Investigations of Marine Teleosts: The Myctophidae, A Case Study. 1974 Berlin, Heidelberg. Springer Berlin Heidelberg, 605-607.

NEILSON, J. & PERRY, R. 1990. Diel vertical migrations of marine fishes: an obligate or facultative process? *Advances in marine biology.* Elsevier.

NORHEIM, E., KLEVJER, T. A. & AKSNES, D. L. 2016. Evidence for light-controlled migration amplitude of a sound scattering layer in the Norwegian Sea. *Marine Ecology Progress Series,* 551**,** 45-52.

OHMAN, M. D., FROST, B. W. & COHEN, E. B. 1983. Reverse Diel Vertical Migration: An Escape from Invertebrate Predators. *Science,* 220**,** 1404-1407.

OLIVAR, M. P., HULLEY, P. A., CASTELLÓN, A., EMELIANOV, M., LÓPEZ, C., TUSET, V. M., CONTRERAS, T. & MOLÍ, B. 2017. Mesopelagic fishes across the tropical and equatorial Atlantic: Biogeographical and vertical patterns. *Progress in Oceanography,* 151**,** 116-137.

PEARRE, S. 2003. Eat and run? The hunger/satiation hypothesis in vertical migration: history, evidence and consequences. *Biological Reviews,* 78**,** 1-79.

PRIHARTATO, P. K., AKSNES, D. L. & KAARTVEDT, S. 2015. Seasonal patterns in the nocturnal distribution and behavior of the mesopelagic fish Maurolicus muelleri at high latitudes. *Marine Ecology Progress Series,* 521**,** 189-200.

PROUD, R., HANDEGARD, N. O., KLOSER, R. J., COX, M. J. & BRIERLEY, A. S. 2018. From siphonophores to deep scattering layers: uncertainty ranges for the estimation of global mesopelagic fish biomass. *ICES Journal of Marine Science*.

RASMUSSEN, O. & GISKE, J. 1994. Life-history parameters and vertical distribution of Maurolicus muelleri in Masfjorden in summer. *Marine Biology,* 120**,** 649-664.

ROE, H. 1983. Vertical distributions of euphausiids and fish in relation to light intensity in the Northeastern Atlantic. *Marine Biology,* 77**,** 287-298.

RUSSELL, F. 1931. The vertical distribution of marine macroplankton. X. Notes on the behaviour of Sagitta in the Plymouth area. *Journal of the Marine Biological Association of the United Kingdom,* 17**,** 391-414.

RØSTAD, A., KAARTVEDT, S. & AKSNES, D. L. 2016. Light comfort zones of mesopelagic acoustic scattering layers in two contrasting optical environments. *Deep Sea Research Part I: Oceanographic Research Papers,* 113**,** 1-6.

SAMEOTO, D. 1988. Feeding of lantern fish Benthosema glaciale off the Nova Scotia Shelf. *Marine ecology progress series. Oldendorf,* 44**,** 113-129.

SAMEOTO, D. 1989. Feeding ecology of the lantern fish Benthosema glaciale in a subarctic region. *Polar Biology,* 9**,** 169-178.

SCHEUERELL, M. D. & SCHINDLER, D. E. 2003. DIEL VERTICAL MIGRATION BY JUVENILE SOCKEYE SALMON: EMPIRICAL EVIDENCE FOR THE ANTIPREDATION WINDOW. *Ecology,* 84**,** 1713-1720.

STABY, A. & AKSNES, D. L. 2011. Follow the light-diurnal and seasonal variations in vertical distribution of the mesopelagic fish Maurolicus muelleri. *Marine Ecology Progress Series,* 422**,** 265-273.

STABY, A., RØSTAD, A. & KAARTVEDT, S. 2011. Long-term acoustical observations of the mesopelagic fish Maurolicus muelleri reveal novel and varied vertical migration patterns. *Marine Ecology Progress Series,* 441**,** 241-255.

WARRANT, E. J. & ADAM LOCKET, N. 2004. Vision in the deep sea. *Biological Reviews,* 79**,** 671-712.

WIEBE, P., MORTON, A., BRADLEY, A., BACKUS, R., CRADDOCK, J., BARBER, V., COWLES, T. & FLIERL, G. D. 1985. New development in the MOCNESS, an apparatus for sampling zooplankton and micronekton. *Marine Biology,* 87**,** 313-323.

WURTSBAUGH, W. A. & NEVERMAN, D. 1988. Post-feeding thermotaxis and daily vertical migration in a larval fish. *Nature,* 333**,** 846.